Interreg
EUROPEAN UNION
North-West Europe
DGE-ROLLOUT

Techno-economic feasibility of geothermal district heating in Lommel and Bree (Belgium)

Deliverables D.T3.4.3 to D.T3.4.12

Ben Laenen & Lien Poelmans (VITO)

vito

Nuhma
Het Limburgs klimaatbedrijf

provincie Limburg

31.12.2022

Contents

List of Figures

List of Tables

Summary

There is a large potential for the development of deep geothermal energy in the INTERREG NWE area. The viability of a geothermal project strongly depends on the amount of heat that can delivered to the customers.

In the present report, a template to evaluate geothermal district heating is provided, that takes the long-term variability into account. In the next chapters, the template is used to evaluate the techno-economic viability of geothermal heating in Bree and Lommel (province of Limburg, Belgium). The objective of this exercise is to evaluate whether there are locations within the two municipalities that may be eligible for the development of deep geothermal district heating. It is a first step in the evaluation of the techno- and socio-economic viability of a potential geothermal project.

Geothermal potential

The main target layer for geothermal projects in Bree and Lommel are sandstones of the Triassic Buntsandstein Formation. The sandstones have moderate to good properties for the development of geothermal doublets. In most of the area, a flow rate of 24 kg/s or more per doublet should be achievable. The expected production temperatures are in the range of 25 to 65°C.

In Bree, another potential geothermal target are sandstones of the Upper Carboniferous Neeroeteren Formation. These sandstones are up to 300 m thick, and core data point to good reservoir properties. However, due to the lack of data about the thickness and reservoir properties of the sandstones over a large part of the study area, the Neeroeteren Formation was not included in this evaluation.

According to literature, limestones and dolomites of Lower Carboniferous age may form a geothermal target in the northern part of Limburg. Both in Bree and Lommel the top of the Lower Carboniferous Limestone Group is situated a depth of -4000 m TAW or more. Below 4000 m, the p10 value of the predicted thermal output of drops below 10 MW. Based on these results and based on the current knowledge about the reservoir properties of the Lower Carboniferous Limestone Group, 3500 m is taken as the depth limit for geothermal projects targeting the lime- and dolostones. For this reason, the limestones were not further considered in the evaluation.

Options for energy cascading

As the expected production temperature of a geothermal system targeting the Triassic sandstones is below 65°C, the options for energy cascading are limited. Low temperature heating is an option, but in most cases the temperature needs to be lifted using heat pumps, even for domestic district heating. The use of geothermal hence is expected be as a heat source for district heating and applications that need low temperature heat.

A typical geothermal plant targeting the Triassic sandstones will use a heat-pump to lift the temperature of the geothermal brine that reached the heat exchanger to the application temperature. For the current evaluation we considered geothermal district heating with a supply temperature of 65°C and a return temperature of 45°C. In case the geothermal brine is hot enough, a pre-heater

(additional heat exchanger) is included to increase the temperature of the return before it enters the heat pump.

The preferred locations for geothermal plants were defined using a spatial optimization model and a cost model for the typical geothermal plant. For each possible location, the model calculates the costs and benefits of supplying heat on an annual basis over the lifetime of a project. The project lifetime was set at 30 years. The result is a map showing locations for profitable geothermal plants and connects them to heat users.

The benefits of the geothermal plants correspond to the revenues from the delivered heat. In this study, two scenarios were considered: a low scenario with a heat price of 40 Euro/MWh, and a high scenario with a heat price of 100 Euro/MWh.

In the low scenario, the optimization tool finds profitable locations for a geothermal plant in both Lommel and Bree. All profitable cases couple a geothermal plant with one or a few large heat users (> 2,000 MWh/year). The most profitable plants are connected to the holiday parks De Vossemeren and Erperheide. In case the heat demand is high enough, the geothermal plant can be located at a preferred geological location at several kilometers distance.

In the scenario with a heating price of 100 Euro/MWh, more profitable geothermal plants are placed. Most of the geothermal plants are connected to one or a few industrial users with a high to moderate heat demand (> 1,000 MWh/year). In addition, cases for geothermal district heating appear in the centers of Bree, Bocholt and Meeuwen. However, for clusters that only contain small heat users (e.g., houses), the cost for the heating network in most cases is too high to result in profitable cases.

1. Introduction

The resource mapping (see D.T1.1.5) and the market/investor correlation (see D.T1.2.2) performed in the context of DGE-ROLLOUT indicate that there is a large potential for the development of deep geothermal energy in the INTERREG NWE area. The viability of a geothermal project strongly depends on the amount of heat that can be delivered to the customers. In case of industrial applications with a large heat demand, heat delivery can be almost year-round. Moreover, the business case for the geothermal plant will be defined by the conditions that are negotiated with one or a few companies. In the case of heat supply to a district heating grid, it is more difficult to come to a feasible business case. In these cases, heat demand fluctuates strongly over the year, and the demand will grow or decline with evolutions within the district heating systems. A template to evaluate geothermal district heating must take the short- and long-term variability into account.

Energy cascading strategies can maximize the energetic efficiency of any geothermal system. This is even more the case for district heating, as it can significantly increase the amount of heat that is delivered by the geothermal plant. Energy cascading corresponds to a stepped use of heat in function of the temperature; subsequent energy demanding processes are fed by excess energy from a previous step.

The current report provides a template to evaluate the feasibility of geothermal district heating. It is based on research that was performed by VITO in the context of EFRO project 910: GEOTHERMIE 2020 [1] and on results of activities 1, 2 and 3.

Chapter 2 gives a description of the template. The template is meant to provide guidance to locate sites where geothermal energy can be profitable. It includes a high-level feasibility evaluation of geothermal district heating in a certain area based on local geology, heat demand and socio-economic conditions. As such, it is tool to identify possible business cases for geothermal district heating. The template can be adapted to the local conditions and to the level of information that is available.

In chapters 3 and 4, we apply the template to find out whether there are locations in the municipalities of Lommel and Bree (Belgium) where geothermal energy can be profitable.

[1] Geothermie 2020 | VITO

2. Template for geothermal district heating

2.1 Objectives

- Briefly describe the objectives of the geothermal project.
- Briefly describe to status of the project and the level of detail of the present evaluation.

2.2 Area of interest

- Briefly describe the target area of the geothermal project including the intended use of the geothermal energy and the main stakeholders.
- Include a map of the area of interest.

2.3 Geological conditions

- Give an overview of the observations (e.g., offset well, seismic campaigns, MT and gravimetric surveys, surface manifestations), data sets and geological models that are used for the evaluation.
- Describe the regional geological conditions that are relevant for the project, covering:
    - The local structural setting;
    - The lithostratigraphic framework;
    - The geothermal gradient and/or local heat flux.
- Describe the geothermal target(s). For each (potential) target provide information the topics listed next. Evaluate the uncertainty and identify knowledge gaps.
    - Depth and thickness;
    - The temperature range;
    - The expected reservoir properties (lithology, porosity, permeability, thermal and mechanical properties if available);
    - The geothermal potential.
- Describe the work program to fill in crucial knowledge gaps and to (further) explore the geothermal potential
- Describe the geological risks that are associated with the development and exploitation of the geothermal potential and define mitigation measures. A bow-tie analysis can be used for a project specific risk assessment and to define mitigating measures [2].

For reservoir properties also consider thermal and rock mechanical properties as these are important to evaluate drilling and exploitation risks.

Geological risks should be linked to the local geological conditions and the characteristics of the geothermal project (e.g., target depth, production temperature, co-production of gasses or other components). General assessments of risks related with deep geothermal can be found in:

- *GEORISK -Inventory and Assessment of Risks Associated to the Development of Deep Geothermal Heating and Power Projects*
- *The DAGO HSE management system* [3]

[2] The bowtie method - CGE Barrier Based Risk Management Knowledge base (cgerisk.com)

[3] www.kasalsenergiebron.nl/content/user_upload/Geothermal_Wells_integrity_study_report_final.pdf

- *KEM-06 Hazard and risk assessment for Ultra Deep Geothermal Energy (UDG) and inventory of preventive and mitigation measures including a quick scan tool*
- scan_dinantian_generic_hazard_inventory_for_drilling_udg_report.pdf (nlog.nl)
- *GEOENVI - Report on environmental concerns: Overall state of the art on deep geothermal environmental data*

2.4 Surface conditions

- Describe the local heat demand:
  - Make an inventory of the current local heat demand;
  - If relevant, make an assessment of the evolution of the heat demand taking into account expected changes in land use, demography, building standards and/or heating technology.
- Describe the options for energy cascading:
  - Make an inventory of options for energy cascading taking into account the local heat demand and/or co-generation.
- Describe the permitting procedure:
  - Make an inventory of the local permitting process and the current state of the project with respect to permitting;
  - Make an assessment of the time needed to obtain the (remaining) permits;
  - Make an inventory of existing permits for geothermal and/or other subsurface activities that require a permit (e.g., oil & gas exploration and exploitation, underground gas storage).
- Describe the surface related risks that are associated with the development and exploitation of the geothermal potential and define mitigation measures. These risks can be technical/environmental as well as non-technical (e.g., permitting, social acceptance).

A map of the spatial distribution of the heat demand in the NWE area is provided in Deliverable T1 2.1.

2.5 Techno-economic assessment

- Describe the geothermal system including both subsurface and surface installation, taking not account connection to the heat demand and cascading options;
- Describe the work program for the development of the geothermal potential and the construction of the geothermal installations taking into account any (further) exploration phases, permitting, financing rounds and lead times.
- Describe the cost model for the geothermal project. The level of detail will depend on the status of the project. It should at least contain costs for:
  - Any further exploration;
  - Development of the well field;
  - Construction of the surface installation;
  - Connection to the heat customers;
  - Measures to mitigate geological risks;
  - Financing costs;
  - Permitting costs;
  - Maintenance cost;
  - Operational costs;

    - One-time incomes and operational subsidies;
    - Revenues.
- Describe the financial risks and possible mitigation measures.

Kostenonderzoek geothermie SDE+ 2018 (pbl.nl) gives an overview of the costs of geothermal energy in the Netherlands.

Information about the CAPEX and OPEX of the Balmatt geothermal plant (Mol, Belgium) is given in Deliverable LT2.1: DGE Guidance Concept Report.

A quick scan for geothermal district heating is available from INTERREG Vlaanderen – Nederland project Geoheat.app.

A tool to identify investment hotspots with regard to regional specificities & heterogeneities is provided in Deliverable T1 4.1: Decision making tool.

3. Techno-economic feasibility of geothermal district heating in Bree

3.1 Objectives

The objective of this exercise is to evaluate whether there are locations within the municipality of Bree (province of Limburg, Belgium) that may be eligible for the development of deep geothermal district heating. It is a first step in the evaluation of the techno- and socio-economic viability of a potential geothermal project in Bree.

3.2 Area of interest

The area that is screened for possible locations for geothermal district heating coincides with the territory of the municipality of Bree. The study area covers 64.96 km². Most of the population lives in and near the town of Bree. Most of the industrial activity is concentrated in the industrial areas Kanaal-Zuid and Kanaal-Noord. Both industrial areas are located east of the city of Bree (Figure 1).

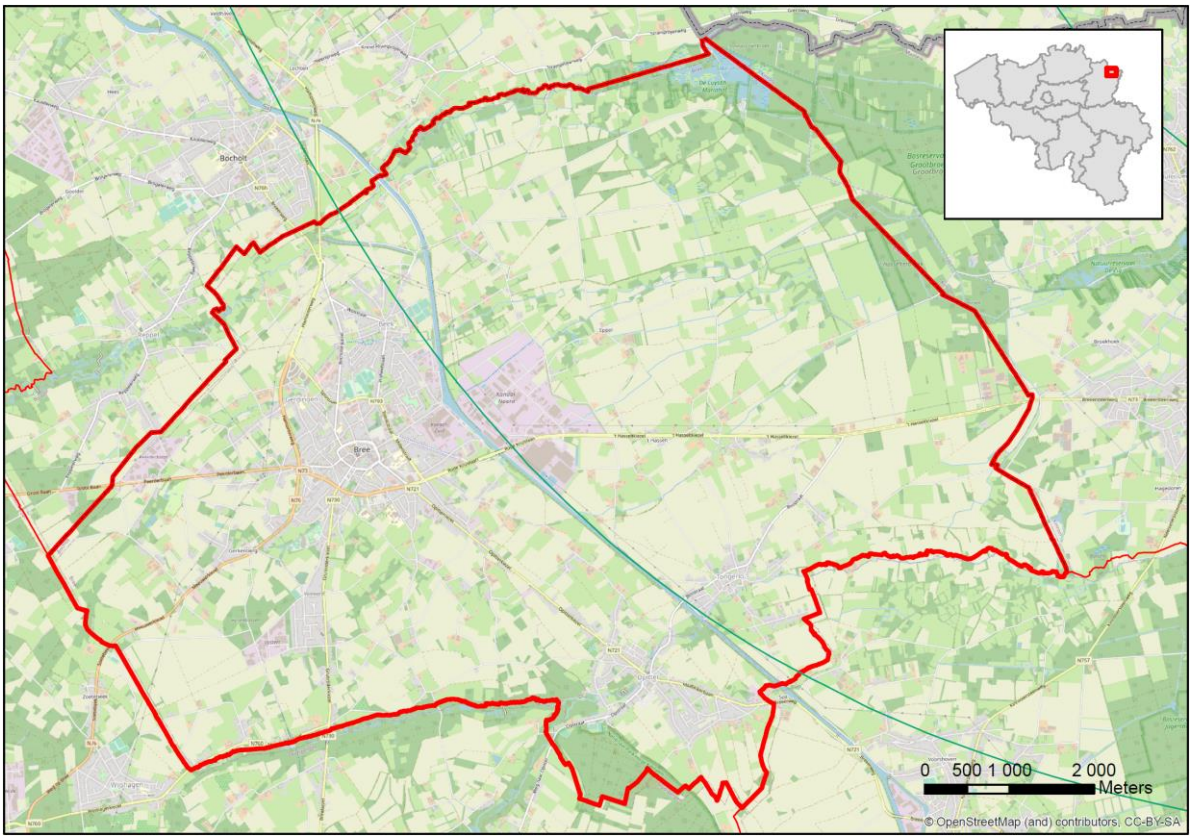

Figure 1: Map of the area that is screened for possible locations for geothermal district heating in Bree, showing many locations of habitation and industrial activity

3.3 Geological conditions

3.3.1 Used data

Wells

Table 1 gives an overview of the wells that were used in the evaluation. Only well 048E0321 lies within the study area. The total depth of this well is 233 m. Information about the lithostratigraphy and characteristics of deeper geological strata was derived from wells outside the study area. The data was extrapolated based on observed depth trends and the 3D Geological Model of Flanders (Geologisch 3D-model G3Dv3 | DOV (vlaanderen.be)). The depth trends used for the extrapolations are discussed below.

Stratigraphic information and data from the wells was derived from the Databank Ondergrond Vlaanderen | DOV, the NLog Datacenter and an in-house database of VITO.

Id	Well	X (m)	Y (m)	Z (m TAW)	Total depth (m)
048E0248	Neerglabbeek	238250	199320	71.02	1357
048E0321	Bree	237269	203204	45.44	233
048W0174	Meeuwen	230225	199381	63.75	20
048W0185	Gruitrode-Muisvenner Bemden	233844	199424	71.65	1371
048W0191	Bree	232477	204071	57.7	15
049W0226	Molenbeersel	247649	207767	33.5	1773
063E2018	Opglabbeek-Louwelsbroek	238210	194690	62.33	1342
063E0223	Opoeteren-Den Houw	240545	194697	81.85	1264.7
063E0224	Gruitrode-Ophovenderheide	234040	196262	77.74	1599
HLH-GT-01	Heerlerheide	260015	218350	80.34	692.2
AST-GT-02	Asten-GT-02	247917	230967	30.34	1673
NDW-01	Nederweert-01	247668	223253	34.48	2942.5

Table 1: Wells used to locate potential sites for geothermal district heating in Bree. Coordinates are in Lambert 1972.

Datasets

Next to the wells shown in Table 1, the following datasets were consulted:

- '*Compilatie en Duiding van Warmtedata in de Diepe Ondergrond van Vlaanderen en Opmaak van een Warmtefluxkaart*': A compilation of temperature data of the Flemish subsurface commissioned by the Flemish Planning Office for the Environment (VPO)
- DOV Verkenner (vlaanderen.be): Lithological data and data from cores/cuttings available through the database of the Flemish Subsurface.

- Reservoireigenschappen | NLOG: A dataset of historical and more recent quantitative estimates of reservoir properties of lithostratigraphic units in the Dutch deep subsurface based on borehole measurements and cores prepared by TNO.
- NLog_poroperm.xlsx (Boringen | NLOG): A dataset of petrophysical measurements on cores from deep wells created by TNO.

Geological models

Depth and thickness maps were adopted or calculated from the 3D Geological Model of Flanders (Geologisch 3D-model G3Dv3 | DOV (vlaanderen.be))

The temperature model was adopted from the compilation of temperature data of the Flemish subsurface and the heat flux map of Flanders (Broothaers et al., 2020)

3.3.2 Methodology

General approach

The north-eastern part of Limburg has a favorable geological setting for geothermal with permeable formations present at significant depth. Four stratigraphic intervals qualify as potential reservoirs (Berckmans and Vandenberghe, 1998):

- Chalk Group: the porous carbonate rocks of the Maastricht and Houthem formations of Late Cretaceous and Early Palaeocene age;
- German Trias Group: sandstone layers within the Röt and Buntsandstein formations of early Middle to Early Triassic age;
- The Belgian Coal Measures Group: coarse, porous sandstones of the Neeroeteren Formation of Westphalian D age;
- Lower Carboniferous Limestone Group: fractured and locally karstified carbonate rocks of Visean to Tournaisian age.

The present evaluation focusses on the sandstones of the German Trias Group, the Neeroeteren Formation and the carbonate rocks of the Lower Carboniferous Limestone Group. The chalks of the Maastricht and Houthem formations were not included in the analysis as the expected formation temperature is too low for deep geothermal district heating.

We start the evaluation with a description of the temperature model that is used to estimate the formation temperatures. Next, we discuss the geothermal potential of each stratigraphic interval. The discussion starts with a short description of the lithostratigraphic unit. A complete description of the units can be found at National Commission for Stratigraphy Belgium (naturalsciences.be), in Lithostratigrafie van het pre-Tertiair in Vlaanderen. Deel I: post-Dinantiaan | Vlaanderen.be and Lithostratigrafie van het pre-Tertiair in Vlaanderen. Deel II: Dinantiaan & Devoon | Vlaanderen.be. Next, the reservoir properties and the estimated formation temperature are presented. Thickness and depth of the reservoir units are derived from the 3D Geological Model of Flanders. The net-over-gross ratio, porosity and permeability of the reservoir units were estimated from geophysical logs and measurements on core plugs.

Building on these insights, the geothermal potential is defined based on the estimated formation temperature and the expected transmissivity. Areas where the permeability x thickness product is

more than 10^{-11} m^3 (~10 Darcy.m) and the formation temperature is above 65°C are marked as high potential areas. A low potential corresponds to a transmissivity of 10^{-12} m^3 irrespective of the formation temperature.

In a final step, maps of the expected thermal power of a geothermal doublet and pump power is created using correlations of the thermal output at selected locations calculated with DoubletCalc with reservoir properties. The following correlations were used to create the maps:

Equation 1: $$Q = A + B \times kh + C \times d_{mid} + D \times kh \times d_{mid}$$

Equation 2: $$T_{hX} = T_{res} - 10^{A+B\times T_{res}+C \times Log(kh)}$$

Equation 3: $$pp = \frac{Q \times Int(A \times d_{top})}{B}$$

With Q the flow rate in kg/s, T_{hX} the temperature at the heat exchanger (°C), pp the pump power in kW, kh the hydraulic transmissivity in Darcy x m, d_{mid} the depth of the middle of the reservoir and d_{top} de depth of the top of the reservoir. Both depths are in meter below surface.

The constants to calculate the geothermal potential of the Triassic sandstones are given in Table 2.

	A	**B**	**C**	**D**
Flow rate (kg/s)	-37.29	7.473E-1	3.987E-2	-2.514E-4
Production temperature (°C)	6.378E-1	1.164E-2	-7.994E-1	
Pump power (kW)	2.0E-2	6.7925		

Table 2: Correlations used to calculate the geothermal potential for the Triassic sandstones

Calculation of the clay content from geophysical logs

The clay fraction (V_{sh}) was calculated from the total gamma ray log (GR). First, the gamma ray index (IGR) is derived:

Equation 4:

$$0 \leq I_{GR} = \frac{GR_{log} - GR_{min}}{GR_{shale} - GR_{min}} \leq 1$$

With GR_{log} the measured gamma-ray value, GR_{shale} the gamma-ray reading for pure clay(stone) and GR_{min} the value for pure sand(stone) or limestone. GR_{shale} was taken as the lowest value from intervals that were described as claystone in the litholog. For the Permo-Triassic in wells from the Campine area in well NDW-01, GR_{shale} varies between 140 and 160 API. GR_{min} was taken as the maximal value of intervals that were described as pure sandstone. GR_{min} varies from 15 to 30 API.

Larionov's (1969) model for pre-Tertiary rock was used to calculate the shale fraction.

Calculation of the porosity from sonic logs

When available, the sonic log was used to calculate the porosity of the different units. For uncompacted or slightly compacted sediments the sonic porosity (DTPO) was determined from the corrected mixing equation prepared by Wyllie at al. (1956):

Equation 5:

$$DTPO = \frac{\Delta t - \Delta t_{ma}}{\Delta t_{po} - \Delta t_{ma}} \times \frac{1}{B_{cp}}$$

In Equation 5 Δt stands for the measured slowness, Δtma for the slowness of the matrix and Δtpo for the slowness of the pores. The slowness of the pores is determined by the composition of the liquid present in the pores. The value was fixed at 200 µs/ft. Δtma depends on the mineralogy and on the texture of the matrix. Table 3 lists the values used to calculate DTPO.

Table 3: Slowness values used to calculate porosities from sonic logs

Lithology	**unit**	**value**
Pure sandstone	µs/ft	53 – 55
Claystone wells Campine area	µs/ft	100 - 105
Claystone NDW-01	µs/ft	70

B_{cp} is a correction term that compensates for the overestimation of the porosity for uncompacted or poorly compacted sediments. As a rule of thumb, clay layers exhibit an inertia greater than 100 µs/ft in uncompacted or poorly compacted sections. Bcp was equated to the value of inertia in the clay layers divided by 100.

Calculation of the porosity from density logs

When available, the formation density log was used to calculate the porosity of the different units. The formation density log measures the bulk density of the formation. Its main use is to derive the total porosity of the formation. The total porosity of the formation can be calculated in case the density of the matrix and of the pore fluid is known:

Equation 6:

$$\emptyset = \frac{\rho_{ma} - \rho_b}{\rho_{ma} - \rho_{fl}}$$

With ρ_{ma} the matrix density, ρ_{fl} the density of the pore fluid and ρ_b the reading of the formation density log. The matrix density was calculated as the weighted average of the shale fraction and the non-shale fraction:

Equation 7:

$$\rho_{ma} = \rho_z + f_{sh} \times (\rho_{sh} - \rho_z)$$

f_{sh} stands for the shale fraction. It is calculated from the gamma ray log. ρ_{sh} is the density of pure claystone. It was fixed at 2.55 g/cm^3. ρ_z is the density of clean sandstone. It was fixed at 2.70 g/cm^3. Average grain densities measured on core samples from Triassic sandstones in the Campine area and from well NDW-01 vary between 2.68 and 2.72 g/cm^3.

Calculation of the net thickness of productive intervals

Most reservoirs are not homogeneous: intervals with good permeability alternate with intervals with low permeability. Intervals with a high permeability largely determine the productivity of the reservoir. The extent to which an interval contributes to the flow is proportional to the product of the thickness and the permeability of the interval. The product of the ratio of productive intervals over the total thickness of the reservoir, also called the net-gross ratio (N/G), and the average permeability of the productive zones is therefore a good measure of the quality of a geothermal target.

The N/G of the different units was calculated from geophysical logs. The gamma ray log was used to calculate the clay content. Productive zones within a sand- and limestone formation are typically characterized by low clay content. First, Vsh was calculated. Then, the cumulative thickness of all intervals with a clay content of 5% or less was calculated and plotted against the total thickness of the lithostratigraphic unit.

3.3.3 Subsurface model DGE aquifers Bree

Lithostratigraphy

The Quaternary and Tertiary sequence mainly consists of coarse to fine grained siliciclastic sediments. An overview of the Quaternary and Tertiary sequence in the study area is given in Deckers et al. (2014). The succession consists of:

- Meuse group (Quaternary): gravel-containing sands to gravels, locally with aeolian sands of the Ghent Formation above it;
- Kieseloolite Formation and equivalent Mol Formation (Late Miocene to Pliocene and possibly even Quaternary): sand and continental clay/peat;
- Kasterlee Formation (Late Miocene): fine glauconitic sands, found in the northern part of the area. In the south, time-equivalent sand of the Wurfeld Formation is found;
- Diest Formation (Late Miocene): glauconitic sands;
- Bolderberg Formation (Middle Miocene): lignite-containing, coarser sand at the top; surmounted by sands and silts of the newly introduced (not yet formal) Molenbeersel Formation; glauconitic sand at the bottom;
- Veldhoven Formation (Late Oligocene to Early Miocene): fine sometimes clayey sand and sandy clay;
- Eigenbilzen Formation (Oligocene): sand;
- Boom Formation (Early Oligocene): clay and silt;
- Bilzen Formation (Early Oligocene): silt and fine sand;
- Sint-Huibrechts-Herne Formation (Early Oligocene): clay and sand;

- Hannut Formation (Late Paleocene): marly clay, clay to sand at the top and local incision by continental clays and sands of the Tienen Formation. The Eocene represents a hiatus due to erosion during the last Eocene. That erosion also cut into the Hannut Formation, which is therefore locally thin.
- Heers Formation (Middle Paleocene): glauconitic sand and marl;
- Opglabbeek Formation (Early Paleocene): continental clay and sand;
- Houthem Formation (Early Paleocene): calcarenites

Chalk Group

The Chalk Group is mainly made up of carbonate rocks. The majority consists of white, pale yellow, cream and light grey, hard, fine-grained bioclastic limestones and marly limestones. In the south-western part of the study area, the top is situated at a depth of -400 to --500 m TAW (Figure 2). East of the Neeroeteren – Grote-Brogel – Overpelt fault, a depth of -1300 m TAW is reached. The low-lying area is part of the Roer Valley Graben. In the graben the thickness of the Chalk Group ranges from 20 to 30 m. West of the graben, the sequence is up to 250 m thick. The difference in thickness is explained by inversion tectonics during the Upper Cretaceous (Rossa, 1986). As a geothermal target, the Chalk Group probably has too low a matrix permeability at the depths encountered in the study area (see well Asten-2 (Heederik et al., 1989) and the Molenbeersel well (Swennen & Dusar, 1997).

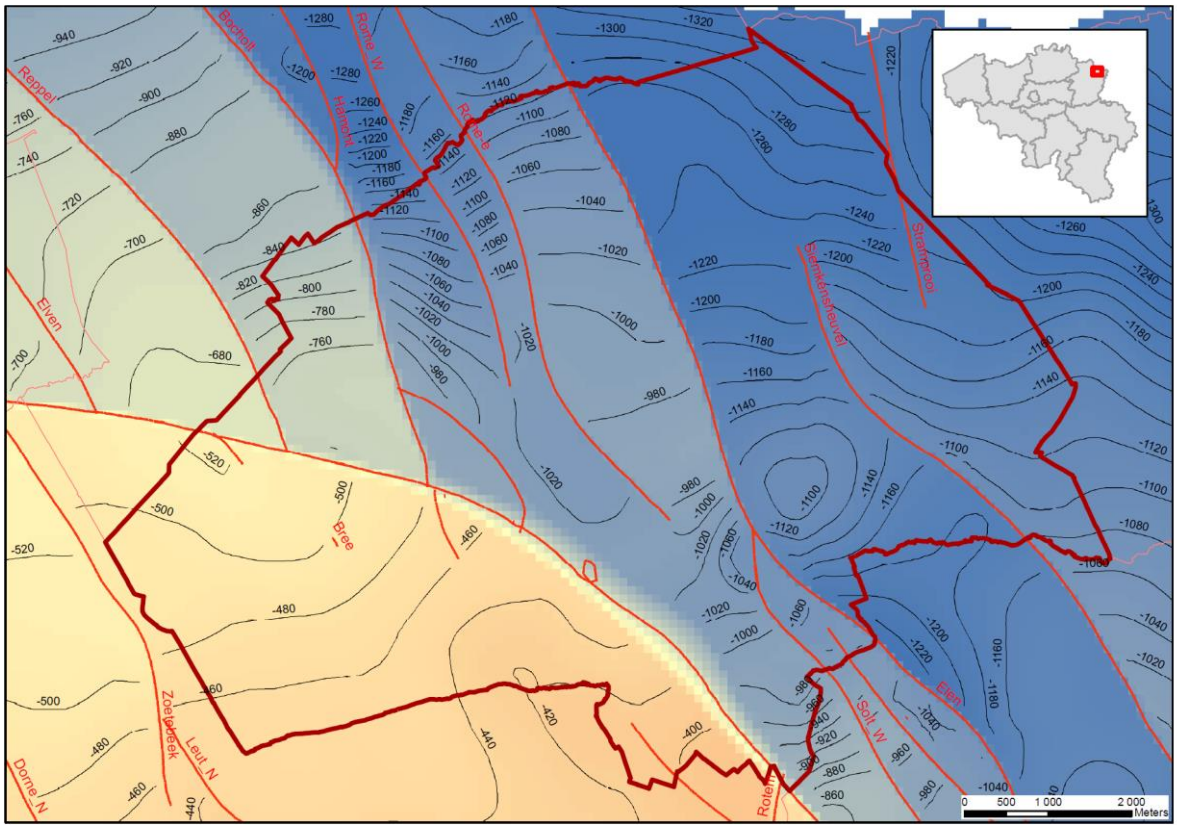

Figure 2: Map of the depth of the top of the Cretaceous (G3D v3.0)

Altena Group

In the eastern part of the study area, east of the Heerlerheide Fault, deposits of the Late-Triassic to Jurassic Altena Group are preserved. The sequence predominantly consists of marine claystones, with sandy and calcareous intercalations (Dusar et al., 2001; Laenen, 2002). The Altena Group is divided in two formations:

- Aalburg Formation: a sequence of dark grey, calcareous, sometimes silty or sandy claystone with thin, clay-rich limestone beds (fossil hash). The formation is rich in pyrite, organic matter, iron oolites and siderite concretions. The base is formed by a characteristic clay-rich limestone interval.
- Sleen Formation: a sequence of grey, fossiliferous claystone. The top is formed by a brown, locally sandy claystone, often rich in megaspores

German Trias Group

Mostly red to variegated siliciclastic sediments, locally rich in anhydrite. The upper part is rich in marl, limestone and dolomite layers. The lower part consists mainly of sand- and siltstones with conglomerate levels. The German Trias Group is of early Middle to Early Triassic age.

- Keuper Formation: an alternation of red-green claystone and clay-rich dolomite to dolomitic marls. The base is sandy and often psammitic. The presence of anhydrite and gypsum layers or nodules is characteristic.
- Muschelkalk Formation: a sequence of grey to mottled marls, clay-rich dolomites and limestones, anhydritic claystones and anhydrite layers.
- Röt Formation: in the study area, the Röt Formation consists of an alternation of reddish brown to greenish, silty and anhydrite rich claystone, and anhydrite. The basal part consists of an alternation of psammitic sand and claystone with thin anhydrite layers. The boundary with the underlying Buntsandstein Formation is difficult to draw due to absence of massive evaporite layers.
- Buntsandstein Formation: a sequence of reddish brown, sometimes mottled siliciclastic deposits ranging from claystone to conglomerate. Locally, the lithology is calcareous. The Buntsandstein is distinguished from the Röt Formation by the scarcity or absence of evaporites and a sandier character.

Helchteren Formation

The Helchteren Formation of Permian age consists of grey, marly sediments and grey, often nodular, clay-rich limestone beds. A red conglomerate layer is often found at the top.

Belgian Coal Measures Group

The Belgian Coal Measures mainly consists of carbonaceous, siliciclastic deposits of Westphalian and Namurian age. The facies evolves from open marine at the base over lower and an upper delta plain to alluvial at the top. In the study area, the group is subdivided in 6 formations:

- Neeroeteren Formation: predominantly consists of pale, massive, partly coarse-grained to conglomeratic sandstones. The pale color is a result of feldspar weathering and the

formation of kaolinite. The sandstones show high porosity and permeability. They are interspersed with brightly colored silt stones and a rare coal seam. The siltstones become more numerous towards the top. The top is eroded everywhere.

- Flénu Formation: consists of a rhythmic sequence of coal, siltstones and sandstones. It contains more coal seams than the underlying Charleroi Formation and the coal seams are generally thicker. Subdivision of the Flénu Formation is possible based on volcanic ash layers and some weak, marine incursions.
- Charleroi Formation: is characterized by a rhythmic succession of coal, siltstones and sandstones. The coal seams are more numerous and thicker than in the underlying Châtelet Formation. The Charleroi Formation can be divided based on the presence of (weak) marine incursions.
- Châtelet Formation: consists of non-marine claystones, siltstones and sandstones in which thin coal layers and root beds occur sporadically. Notwithstanding the low coal content, mineable coal seams are present. The formation can be subdivided based on the presence of goniatite-containing marine layers.
- Andenne Formation: largely consists of a cyclical succession of non-marine, silty claystones and sandstones with thin coal seams and root beds. Thin marine claystone beds with goniatites are found as well as limestone beds. Thick (up to 30 m), bleached, quartzite sandstone bodies occur at different stratigraphic levels.
- Chokier Formation: consists of calcareous claystones and bituminous claystone rich in pyrite (ampelite) and silicate rocks. It contains a rich marine fauna (including goniatites and Posidoniellae).

Lower Carboniferous Limestone Group

The Lower Carboniferous Limestone Group mainly consists of dark grey, grey to beige, limestones and/or dolomites. Locally calcareous clay or sandstone levels occur. The limestones and dolomites are locally karstified. In many places the top is silicified. Chert occurs at certain stratigraphic levels. In the northeast of Limburg, there are no deep wells that reach the limestones. Therefore, the actual nature of the deposits in the area can only be deduced from wells in Dutch Limburg and trends observed along the southern border of the Campine Basin. It is expected that the top of the limestones in the study area consists of thin to thick banked, grey to black limestones and dolomites of the Goeree Formation. Towards the top, the formation becomes clay-rich with the appearance of carbonate-rich or silicified black claystones that grade gradually into the black claystones of the Souvré Formation. The base of the sequence is expected to consist of an alternation of dark grey, partly calcareous claystones, nodular claystones, limestones and grey, sometimes micaceous silt and sandstones that belong to the Bosscheveld Formation. A detailed description of the lithostratigraphy of the Lower Carboniferous Limestone Group in the Campine area is given in Laenen (2003).

Temperature model

In a recent evaluation of temperature data from the Flemish subsurface, Broothaers et al. (2020) show a west to east trend of declining geothermal gradients in the northern part of Belgium. In the Northeast of Limburg, the average temperature is about 21°C at -500 m, 37.5°C at -1000 m and

67.5°C at -2000 m TAW. Considering an average temperature of roughly 10°C in the topmost layers, this corresponds with a geothermal gradient of 0.022°C/m in the shallow strata and 0.031 C/m below -500 m TAW. In most of the wells that have been used to derive the temperature – depth relationship for the area, -500 m TAW more or less corresponds to the top of the Chalk Group. The only exception is well 049W0226 (Molenbeersel). In this well, the top of the Cretaceous is located at -1218 m TAW. The difference in geothermal gradient between the shallow and deep strata can be explained by a difference in average thermal conductivity, and by stronger groundwater flow in the post-Cretaceous sediments.

Broothaers et al. (2020) show that temperature in the uppermost 50 m of the subsurface is constant at 11.0 ± 1.8°C. When discarding measurements from above 0 m TAW, the temperature data reveals a clear linear trend with depth, starting at a temperature of 10.8 ± 1.8°C at 0 m TAW. Based on these observations, the following temperature model is defined for the study area:

For the post-Cretaceous sediments (Equation 8):

$$T_z = 11 - 0.022 \times z$$

For a depth below the top of the Cretaceous (Equation 9):

$$T_z = 11 + 0.009 \times z_{tC} - 0.031 \times z$$

With T_z the temperature at depth z in °C, z_{tc} the depth of the top of the Cretaceous and *z* the depth in meter relative to TAW (negative values are below 0 m TAW).

The model is based on bottom hole temperatures (BHT) measured in wells from the area (Table 1). The BHT readings are not corrected. Most of the measurements were made shortly after (the section of) the well had been drilled. Moreover, the model is not constrained for depths below 1600 m, due to lack of data from deeper formations.

No temperature readings are available for the Carboniferous in the area. The evaluation by Broothaers et al. (2020) shows that the thermal conductivity of the Belgian Coal Measures Group decreases with depth. This results in a steepening of the geothermal gradient. This steepening is most pronounced in the lowermost part of the sequence: the claystone dominated layers at the base of the Andenne formation and the organic rich claystones of the Chokier formation. Consequently, the model is likely to result in an underestimation of the formation temperatures in the Belgian Coal Measures Group and in the Carboniferous Limestone Group.

Potential geothermal reservoirs units

- Buntsandstein Formation

Vandenberghe (1991) identified the Buntsandstein Formation as a potential geothermal target. In the Campine area, the Buntsandstein is divided in 3 members:

- Bree Member: The upper part consists of red to mottled, fine to medium sandstones. Thin gypsum and anhydrite layers may occur near the top, as well as numerous gypsum or anhydrite nodules and gypsum or anhydrite filled veins. The lower part is characterized by

an alternation of shale and sandstone. The color is predominantly red, sometimes mottled or bleached. The sandstones are very fine to medium fine and often calcareous.

- Bullen Member: A monotonous sequence of red to mottled, medium to very coarse sandstones and conglomerates. Locally, fine sandstones and siltstones, as well as calcareous levels occur.
- Gruitrode Member: Red to reddish brown sand- to siltstones. The upper part of the member consists of sand- and siltstones. The sandstones beds range from very fine to very coarse. Locally, conglomerate layers occur. The lower part of the member consists of siltstones with calcareous nodules and fine sandstone intercalations. Near the top of the lower unit paleosols occur.

The Bullen Member and the upper, sandy part of the Gruitrode Member are an equivalent of the Dutch Nederweert Sandstone Formation (Nederweert Sandstone Formation | DINOloket). The sandstones of the Buntsandstein Formation have been marked as potential geothermal reservoirs in the northeastern part of Limburg as well as in Dutch Limburg and Noord-Brabant (Milius, 1983; Vandenberghe, 1991; Berckmans & Vandenberghe, 1998). Based on the succession found in wells in and near the study area, two reservoir levels can be identified: the sandstones of the Bree Member and the sandstones of the Bullen Member and the upper part of the Gruitrode Member (Nederweert Sandstone).

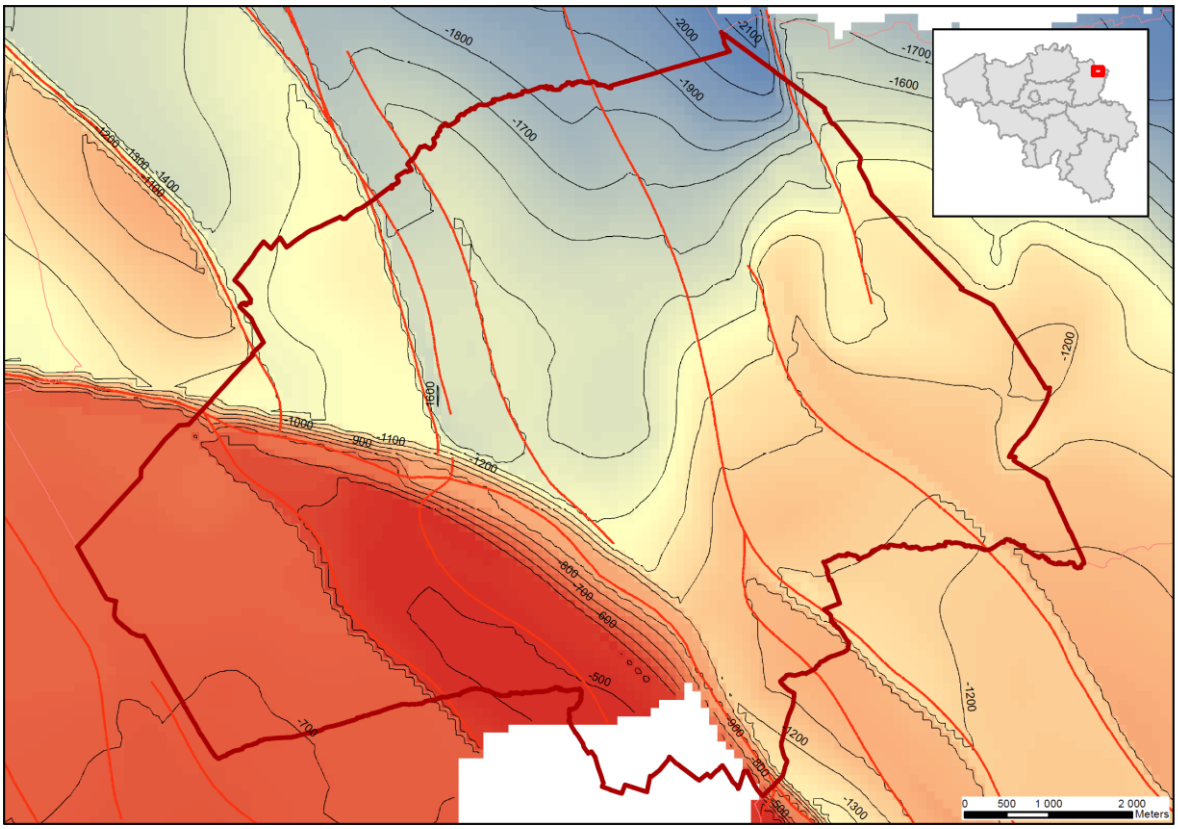

Figure 3: Map of the depth of the top of the Buntsandstein Formation (based on G3D v3.0)

West of the Neeroeteren – Grote-Brogel Oost – Overpelt fault zone, the top of the Buntsandstein Formation is situated at a depth of -500 to -750 m TAW (Figure 3). The area is subdivided in two parts: the 'Bree high': a structural high that is enclosed by the Bree fault and the Neeroeteren – Grote-Brogel Oost – Overpelt fault zone, and the low-lying area west of it. In the Roer Valley

Graben, the top of the Buntsandstein Formation is situated at a depth between -1200 and -2000 m TAW. In the graben, the top of the Buntsandstein Formation dips gradually towards the north-northeast. This trend is transected by a number of normal faults with throws of the order of 10 to 60 m.

- Neeroeteren Formation

Vandenberghe (1991) states that the sandstones of the Neeroeteren Formation form a small geothermal reservoir in the northeast of the Campine Basin. The sandstones have only been drilled in the northeastern part of the Campine basin west of the Heerlerheide Fault (Langenaeker, 2000). The thickest section of the Neeroeteren Formation was encountered in borehole 048E0248 (KB146 – Neerglabbeek): the drilled thickness measured 283 m, the stratigraphic thickness 275 m (Dusar & Houlleberghs, 1981). Seismic data suggest that the sandstones may be present east of the Heerlerheide Fault as well. The thickness of the sequence may reach a few hundred meters locally.

West of the Neeroeteren – Grote-Brogel Oost – Overpelt fault zone, the top of the Upper-Carboniferous is situated at a depth of -600 to -1300 m TAW (Figure 4). The area can be split in 2 parts: a structural high known as 'Hoog van Bree') that is enclosed by the Neeroeteren – Grote-Brogel Oost – Overpelt fault zone and the Bree fault, and a low-lying area west of it. Across the Neeroeteren – Grote-Brogel Oost – Overpelt fault zone, the top of the Upper Carboniferous deepens to -1700 - -1800 m TAW. In the graben, the top of the Upper Carboniferous deepens towards the northeast. It reaches a dept of -2500 m in the northeastern corner of the study area. The area is transected by a number of north-northwest – south-southeast trending normal faults. Throws along these faults are of the order of 50 – 150 m.

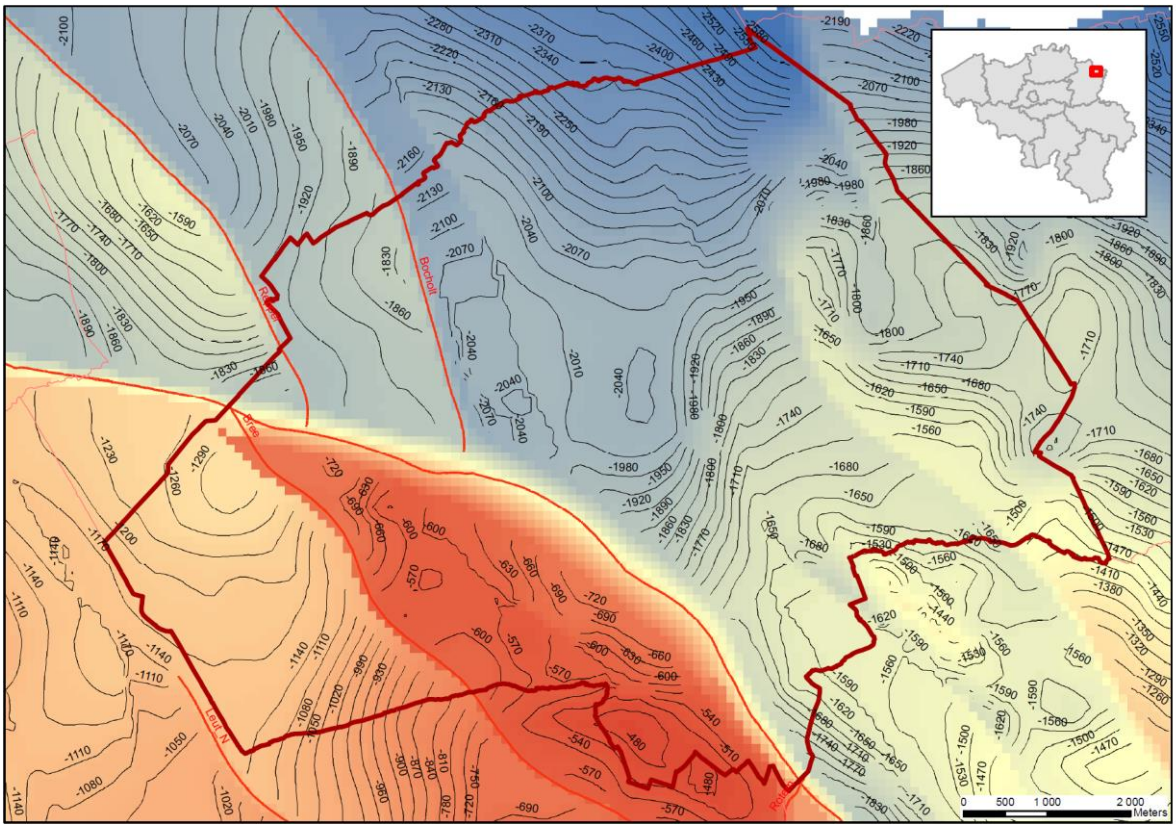

Figure 4: Map of the depth of the top of the Upper Carboniferous (G3D v3.0)

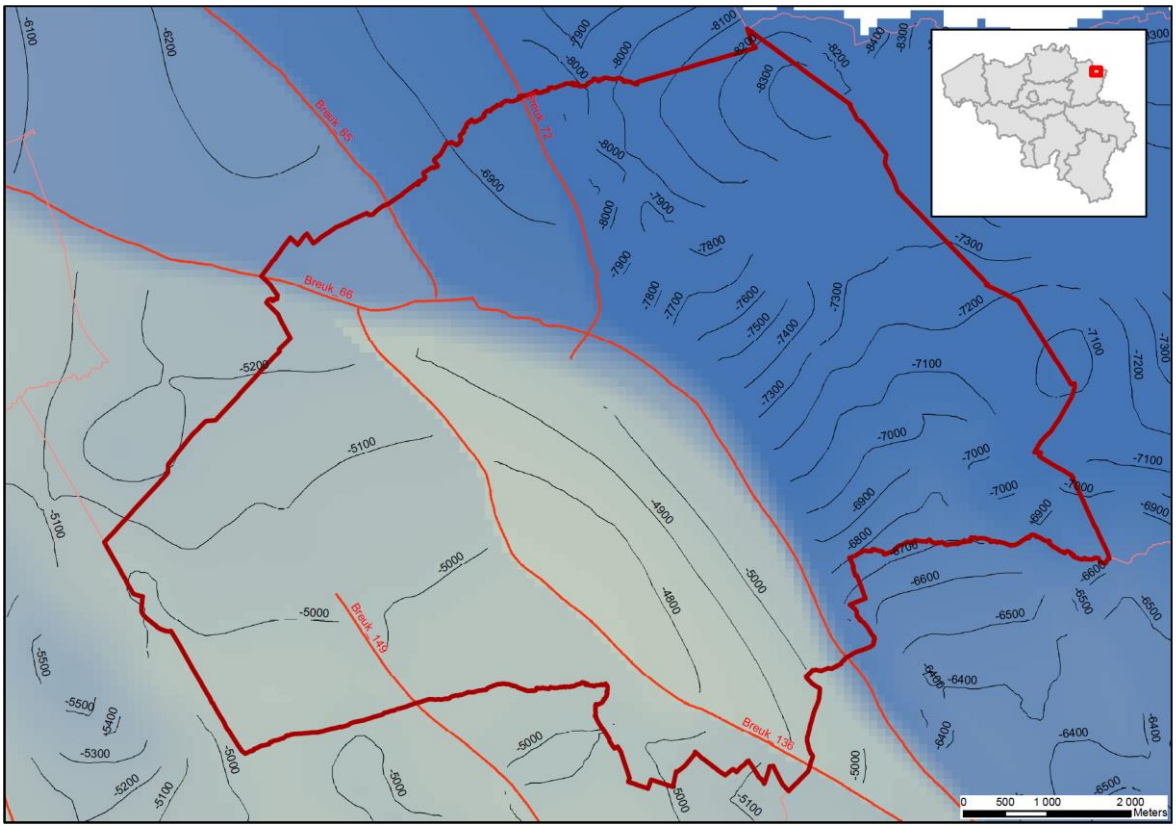

Figure 5: Map of the depth of the top of the Lower Carboniferous (G3D v3.0)

- Lower Carboniferous Limestone Group

The karstified and fissured limestones and dolomites of the Carboniferous Limestone Group are marked as a regional geothermal reservoir in the Campine area (Vandenberghe, 1991; Berckmans & Vandenberghe, 1998; Broothaers et al., 2021). The Lower Carboniferous Limestone Group however has never been drilled in the vicinity of the study area. The geothermal potential of the sequence hence can only be deduced by extrapolation of data from well that were drilled in the western part of the Campine area.

In the study area the top of the Lower Carboniferous sequence is situated at a depth that ranges from -4800 on the 'Bree high' to -8300 m TAW in the Roer Valley Graben (Figure 5). Across the Neeroeteren – Grote-Brogel Oost – Overpelt fault depth changes by about 1500 m. In the graben, the top of the Lower Carboniferous deepens gradually towards the north – northeast. This trend is transected by a number of north-northwest – south-southeast trending normal faults.

3.3.4 Geothermal potential of the Buntsandstein Formation

Depth and thickness

In the study area the top of the Buntsandstein Formation is located at -500 to -1800 m TAW (Figure 3). In the wells that penetrated the Buntsandstein in the Campine area, the thickness ranges from 1 to 566 m (Table 4). All wells that penetrate the Buntsandstein Formation in the Campine area are situated west of the Neeroeteren – Grote-Brogel Oost – Overpelt fault zone. In places where the

entire sequence is preserved, the thickness of the Bree Member is about 190 m. The thickness of the Bullen Member varies between 210 and 230 m. The thickness of the Gruitrode Member varies more: from 38 m in well 063W200 to 94 m in well 047E196. The member becomes thicker towards the northwest.

Table 4: Thickness of the Bundsandstein Formation and Helchteren Formation in wells from the Campine area

Well		**Thickness (m)**				
BGD Arch	KB	Buntsandstein Fm	Bree Mbr	Bullen Mbr	Gruitrode Mbr	Helchteren Fm
47W262	179	5			5	
47W264	186	20			20	
47E196	174	103		9	94	15
62E273	177	1			1	25
62E281	197	3			3	
92E004	60	151		62	89	24
62E276	183	297		230	67	31
62E290	206	91		40	51	28
63W007	30	14			14	
63W200	121	201		163	38	30
48W172	98	227	31	196		
48W185	169	321	53	210	58	30
48W191	201	448	163	222	63	39
63E224	172	137		83	54	13
63E225	173	26			26	20
63E002	40	161	10	151		
63E001	6	42		42		
63E218	161	27			27	8
64W215	99	264	264			
64W004	31	292	292			
46W174	64	566	220		346	40

The thickness of the Buntsandstein Formation within the graben is estimated from the seismic survey 2007 - Bree - Kinrooi – Maaseik (Laenen et al., 2008). The average two-way-travel time (TWT) of section between the Röt Formation and Gruitrode Member is 194 ms (75% quartile 229 ms). Assuming an interval velocity of 3600m/s, this corresponds to a thickness of 350 m (75% quadrille 410 m). The interval between the top of Gruitrode and the top of the Upper Carboniferous measures on average 79 ms (75% quartile 97 ms). Assuming an interval velocity of 3600m/s, this corresponds to a thickness of 140 m (75% quartile 175 m). This interval includes the silt- and claystone dominated lower part of the Gruitrode Member and the Helchteren Formation. In the wells, the Helchteren Formation is up to 40 m thick. Assuming an average thickness of 40 m for the Helchteren Formation, the thickness of the Buntsandstein Formation in the graben is estimated to be 450 m (75% quadrille 545 m). The estimated thickness values are in line with the well observations.

To create the thickness maps of the productive intervals, we assumed that the Bree Member has a maximal thickness of 190 m. The maximal thickness of the Bullen Member plus the sandy upper part of the Gruitrode Member (Nederweert equivalent) was set at 285 m.

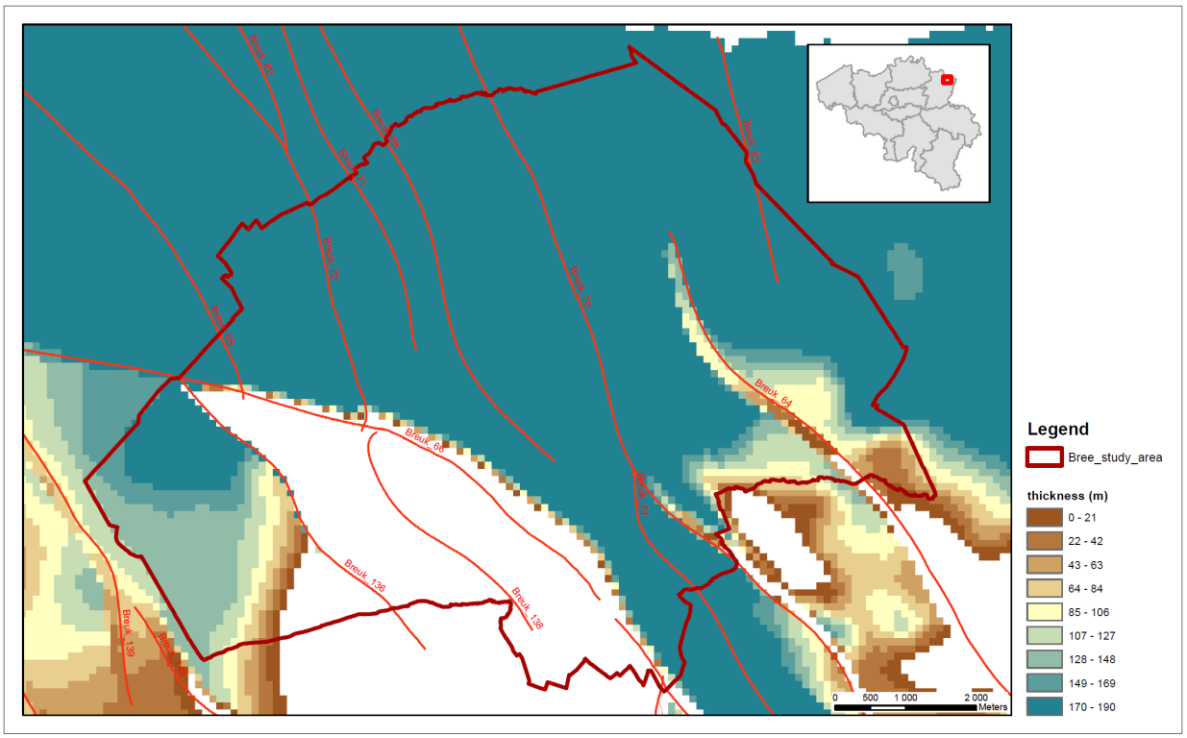

Figure 6: Thickness of the Bree Member in the study area.

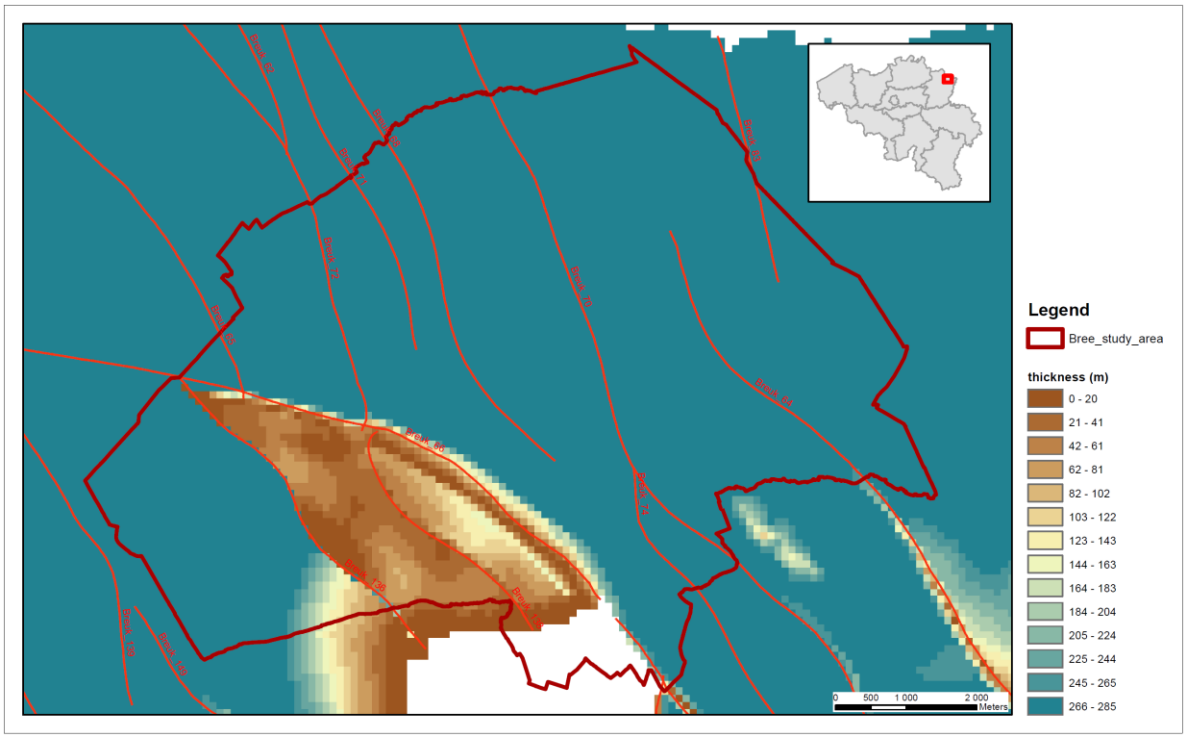

Figure 7: Thickness of the Bullen Member and sandy part of the Gruitrode Member (Nederweert equivalent) in the study area

In the study area, the formation is thinnest on top of the Bree high. Here, the upper part of the formation has been eroded. South of the Bree high, the formation is absent. In the graben, the sequence is (almost) complete and the thickness reaches about 520 m.

In the study area, the entire Bree Member is only preserved within the graben. Here the thickness is about 190 m (Figure 6). The estimate is based on seismic data. West of the Neeroeteren – Grote-Brogel Oost – Overpelt fault zone, the member is partly or totally eroded. On top of the Bree high, the Bree Member is missing.

The combined thickness of the Bullen Member and the sandy upper part of the Gruitrode Member (Nederweert equivalent) in the study area ranges from 0 to 285 m (Figure 7). The thickest sequence is found in the graben and northwest of the Bree high. In these areas, the entire sequence is preserved. On the Bree high and towards to south, the sequence is partly or entirely eroded.

Reservoir properties

Within the Campine area, the Buntsandstein formation has been drilled in 16 boreholes. Geophysical logs and core analyses of 5 of these wells were used in this analysis. In addition, logs and core analyses from the Nederweert formation of the Dutch wells NDW-01, P10-01 and P11-04 were used to derive estimates of the reservoir properties.

Table 5: Thickness and net-over-gross ratio of the different members of the Buntsandstein in well from the Campine area

Well-ID	Stratigraphic unit	thickness	net-over-gross
048W0191	Bree Member (Buntsandstein)	162.9	0.62
048W0185	Bree Member (Buntsandstein)	56	0.879
062E0276	Bullen Member (Buntsandstein)	230	0.92
048W0191	Bullen Member (Buntsandstein)	221.9	0.91
048W0185	Bullen Member (Buntsandstein)	210	1
063E0224	Bullen Member (Buntsandstein)	67.1	0.989
062E0276	Gruitrode Member (Buntsandstein)	66.8	0.506
048W0191	Gruitrode Member (Buntsandstein)	62.9	0.446
048W0185	Gruitrode Member (Buntsandstein)	46.8	0.924
063E0225	Gruitrode Member (Buntsandstein)	22.9	0.452
NDW_01	Rogenstein Laagpakket	42.9	0.102
NDW_01	Nederweert Zandsteen Laagpakket	291.9	0.886

Table 5 shows the net-over-gross ratio of the different members of the Buntsandstein Formation. The values were calculated from sonic and density logs. The net-over-gross ratio of the Bree Member is about 0.7. The member contains silty-shaly intervals and the base is shaly as well. The Bullen member consists of a homogenous sandstone-dominated sequence. Coarse and medium sands are the main lithologies found in the cores of well 063W0200 (Table 6). The homogeneity of the Bullen member is reflected in an average net-over-gross ratio of 0.95. The lithology of the

Gruitrode member is more variable. The top is characterized by sand- and siltstones. The base is silt- and claystone dominated. The heterogeneity of the Gruitrode Member is also reflected in the proportions of the different lithologies derived from core descriptions (Table 6) The heterogeneity results in a net-over-gross ratio that varies between 0.45 to 0.9. The highest value corresponds to the top of the member. It ties in with the overlying sandstones of the Bullen Member. A similar net-over-gross ratio is calculated for the Nederweert Sandstone Member in well NDW-01.

The porosity of the sandstones tends to decrease with depth (Figure 8). Both the core data and the porosity calculated from sonic and density logs reveals a large scatter. This is partly due to differences is sediment typology of the beds, which ranges from very coarse sandstone to claystone. Moreover, the samples and wells show differences in diagenesis (Swennen, 1984; Bertier et al., 2022). Some beds consist of poorly consolidated sands. Other beds are well cemented. The main cement types are quartz and dolomite.

Table 6: Percent fraction of different lithologies within the Gruitrode and Bullen members, based on core descriptions from wells 063E0224 (KB172) and 063W0200 (KB121) respectively

Lithology	**Gruitrode member**	**Bullen member**
Conglomerate	8	6
Coarse sandstone	14	18
Medium sandstone	45	73
Fine sandstone	16	1
Siltstone	6	1
Mudstone	11	0

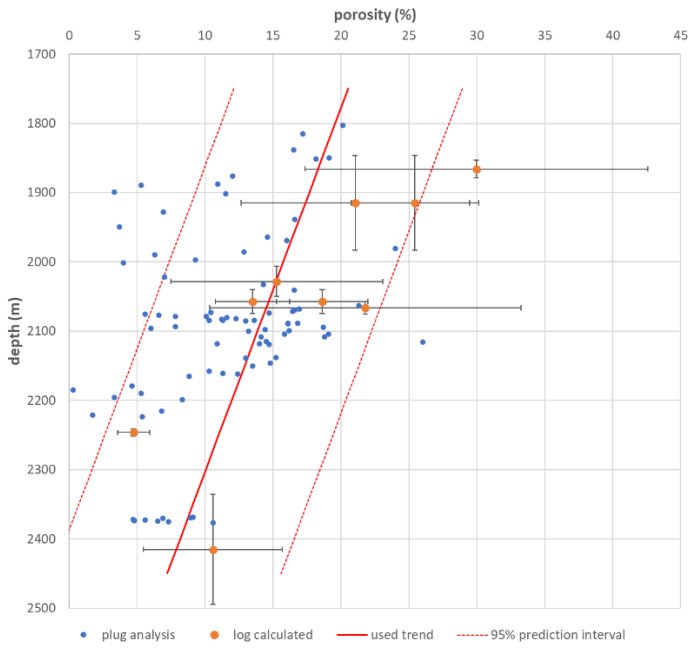

Figure 8: Porosity – depth relationship observed in cores and calculated from geophysical logs from the Buntsandstein Formation in the Campine area (Belgium) and from the Nederweert Formation (Netherlands)

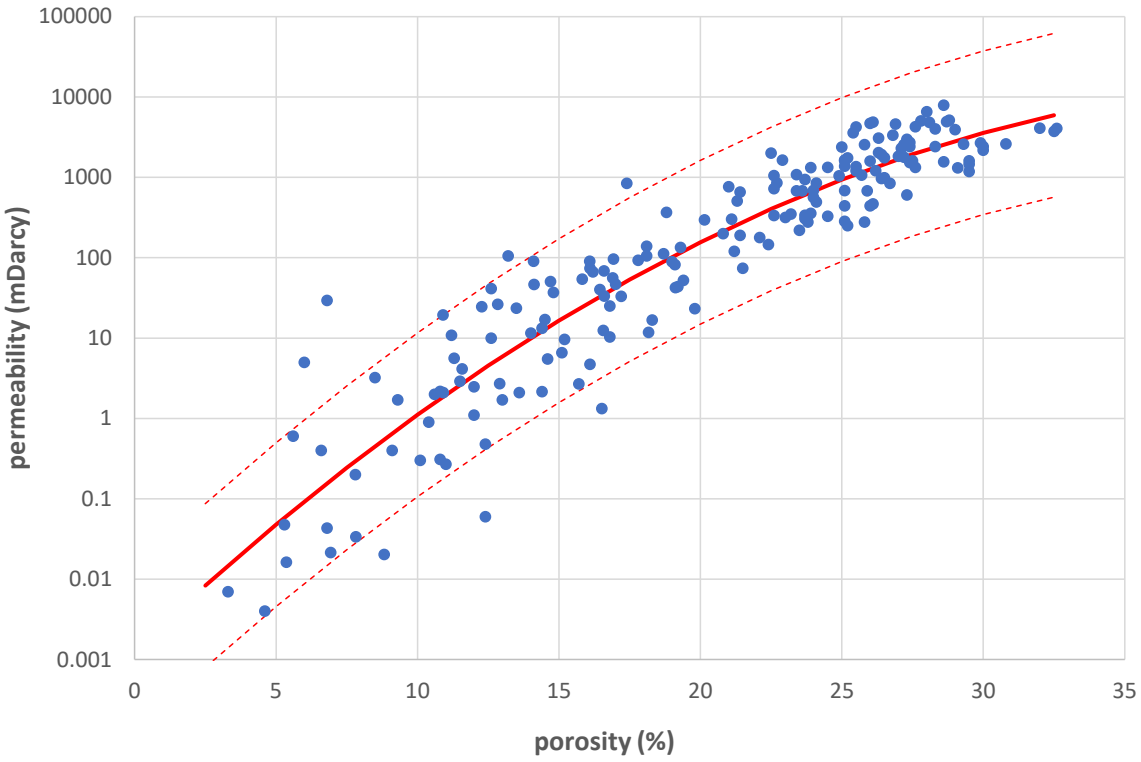

Figure 9: Permeability – porosity relationship derived from core samples from the Buntsandstein Formation from wells drilled in the Campina area and on cores from the Nederweert Formation (Netherlands).

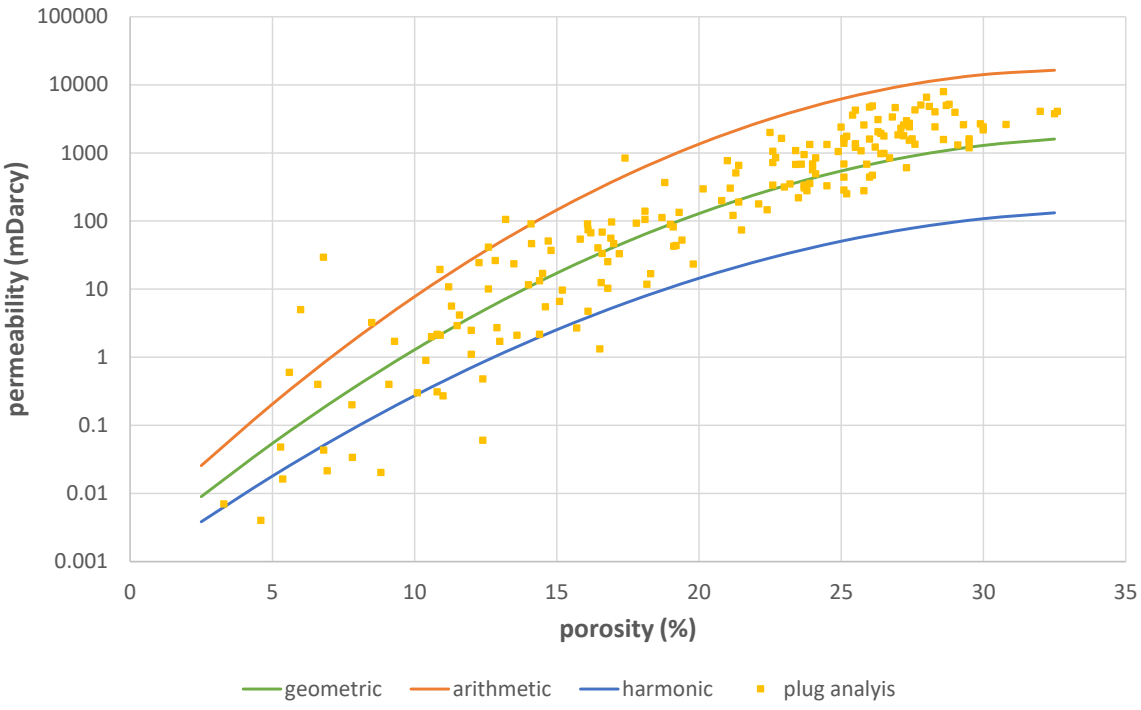

Figure 10: Permeability – porosity relationship derived from density and sonic logs of the Buntsandstein Formation

The permeability of the Buntsandstein Formation measured on core samples ranges from wells that were drilled in the Campine area range from < 0.05 mDarcy to 367 mDarcy. Analyses on cores from the Nederweert Formation range from < 0.2 mDarcy to 7906 mDarcy. Permeability increases with increasing porosity (Figure 9). A similar trend is seen for the single equivalent permeability calculated from sonic and density logs (Figure 10). As the sandstones are heterogeneous with respect to grain size distribution and diagenesis, the single equivalent permeability lays between the harmonic and geometric mean of the permeabilities calculated from the geophysical logs. In case the permeability variations away from a well are unknown, it is reasonable to assume that the equivalent permeability of the sandstone lies between the harmonic and the arithmetic average of the values calculated from the logs (Cardwell & Parson, 1945; Renard & de Marsily, 1997).

Based on the permeability – porosity relationship, layers with a porosity of 15% or more can be expected to have moderate to good flow properties.

In Belgium, the Triassic sandstones have not been developed for geothermal yet. In the western part of the Netherlands, sandstones that are a time-equivalent of the Buntsandstein Formation have been developed as a geothermal resource at Brielle. The resource is located at a depth of 2200 m. The reservoir temperature is 84°C. Pressure transient analyses on the production and injection tests performed on both wells of the doublet point to a productivity between 5.6 and 13 m^3/h.bar and an injectivity of 6.6 m^3/h.bar. Permeability is estimated to be in the range of 110 – 170 mDarcy, assuming that the entire sandstone section is contributing to the flow (Lingen, 2015a; Lingen, 2015b). The geothermal plant of Aardwarmte Vierpolders has been in operation since 2016. It delivers heat to a cluster of greenhouses. Challenges of the project are the co-production of natural gas and inflow of sand.

In another project, Trias Westland explored the geothermal potential of the time-equivalent Lower Germanic Trias Group at Naaldwijk. In exploration well NAALDWIJK-GT-01, the top of the group was reached at a depth of 3790 m. Core analyses revealed porosities in the range of 1.5 – 4% and permeabilities below 0.05 mDarcy. The permeability calculated from geophysical logs ranges from 0.01 to 1.7 mDarcy. The transmissivity of the sandstones was estimated at 0.008 Darcy.m. The sandstones proved to be well cemented with little remaining pore space (see documentation from well NAALDWIJK-GT-01 on Datacenter | NLOG).

The results of the 2 geothermal projects in the Netherlands are in line with porosity and permeability data from Dutch oil and gas wells. The porosity of the sandstones declines as a function of depth. At 3000 m, the average porosity measured on core samples from the Lower Germanic Trias Group is 11 – 12%, at 4000 m 5 – 10%. Based on the permeability-porosity relationship derived from the samples, average permeability at 3000 m is of the order of 5 mDarcy, and at 4000 m 0.5 mDarcy or less.

Core analyses from wells in the Belgian part of the Campine basis suggest a stronger decrease of porosity and permeability with depth than in the Dutch wells (Figure 8). Based on this Belgian data, the sandstones of the Buntsandstein Formation are expected to be a moderate to good geothermal reservoir at depths above 2250 m.

Geothermal potential

The geothermal potential of the Bullen Member and from the Nederweert equivalent was calculated using DoubletCalc v1.4.3. at 17 locations in the study area. The maximal allowed pressure difference was set at:

Equation 10:

$$\Delta P = 2 \times P_{res} \times 0.1$$

With P_{res} the hydrostatic pressure at the top of the reservoir.

The results were used to define a correlation between flow rate and temperature loss with the reservoir properties and well depth. These correlations were used to generate a map of the expected flow rate and production temperature for the 2 stratigraphic intervals.

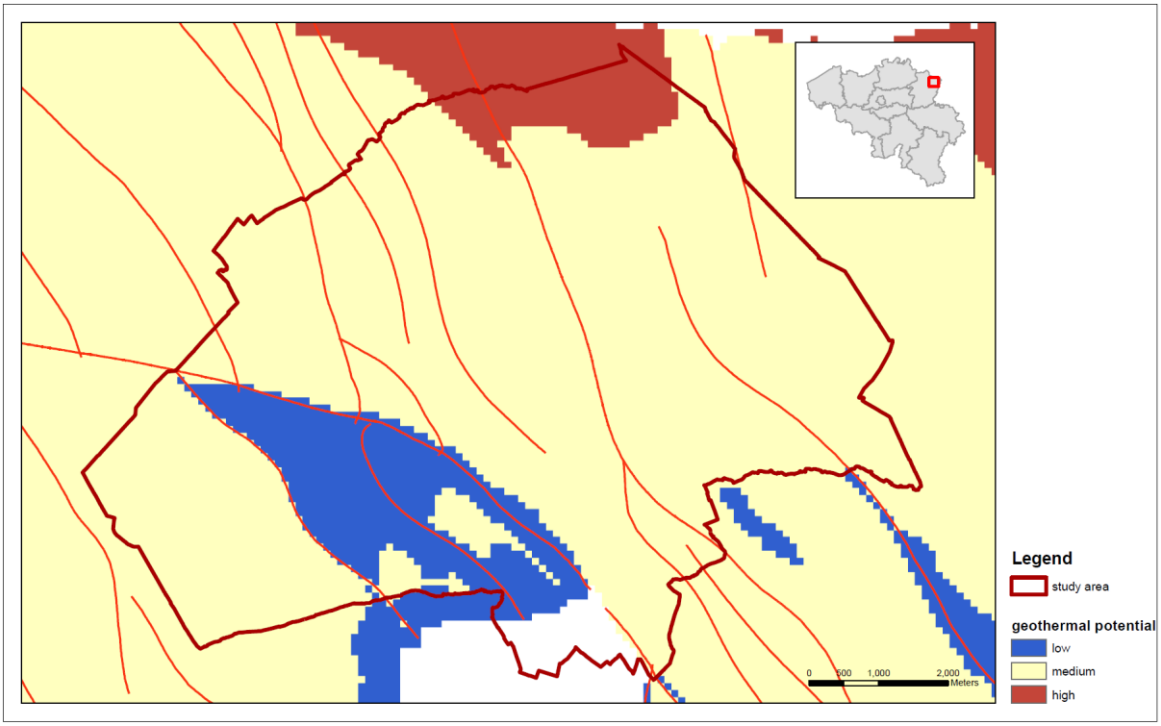

Figure 11: Map of the geothermal potential of the Buntsandstein Formation in the Bree area based on the criteria discussed in the section methodology

The total geothermal potential of the Triassic sandstones was calculated as the average potential of the Bree Member and Nederweert equivalent weighted by flow rate (Figure 11). West of the Neeroeteren – Grote-Brogel Oost – Overpelt fault zone, the geothermal potential is low to moderate. In this area, part of the sandstones is eroded. Moreover, the geothermal resource in this part of the study area only qualifies for low-temperature heating, as the reservoir temperature varies from 20 to 35°C. In the Roer Valley Graben, the geothermal potential is moderate to high. Here, reservoir temperature is between 40 and 65°C. Maps showing the estimated production flow rate for the two stratigraphic sub-units are given in Annex 1. The estimated formation temperature is show in Annex 2.

The productivity of the Triassic sandstones has been tested at two locations: at Meeuwen – Bullen (well 063W0200 – KB121) and at Bree (well 048W0191 – KB201). Well 048W0191 has been drilled in the context of a research program to explore the geothermal potential of the Campine area. An airlift and an injection test were performed to define the geothermal characteristics of the Buntsandstein Formation. The top of the productive interval was located at 1200 m. Analyses of the pressure build-up and fall-off point to a transmissivity of 9 Darcy.m and a productivity of 5.6 m^3/h.bar. A reservoir temperature of 41.5°C was derived from the test results. Well 063W0200 was drilled in the context of coal exploration. Aquifers in the overburden of the coal measures were tested by low-rate pump tests. The top of the Buntsandstein was reached at a depth of 631.8 m, the base at 834.6 m. Analyses of the test results point to a hydraulic conductivity of 0.005 m/d (Patyn, 1999). The productivity index of the Triassic sandstones is estimated at 1.3 m^3/h.bar (Vandenberghe, 1991).

The geothermal potential map predicts a productivity of the geothermal doublet of 3.9 m^3/h.bar at the location of well 048W0191 and of 1.2 m^3/h.bar at the location of well 063W0200. Both figures are in line with the results of the pump tests.

3.3.5 Geothermal potential of the Neeroeteren Formation

Depth and thickness

The Neeroeteren formation has been marked as a geothermal resource in the northeastern part of the Belgium (Vandenberghe, 1991; Berkmans & Vandenberghe, 1998). The sandstones of the Neeroeteren Formation form a small geothermal reservoir in the northeast of the province of Limburg (Vandenberghe, 1991). Figure 4 shows the depth of the top of the Upper Carboniferous in the study area. West of the Heerlerheide Fault, the uppermost layers of the Belgian Coal Measures Group belong to the Neeroeteren Formation. On top of the Bree High, the coal measures are reached at -600 to -700 m below TAW. Further to the west, the top is reached at -700 to -1200 m. The top the sequence dips towards the north. East of the Heerlerheide Fault, the top is located at -1500 to -2200 m TAW, deepening towards the north.

The Neeroeteren Formation has been drilled in 6 wells that are located north of the former eastern mining area west of the Heerlerheide Fault (Wouters & Gullentops, 1988). The thickest section of the Neeroeteren Formation was encountered in the KB146 borehole (Neerglabbeek): the drilled thickness is 283 m, the stratigraphic thickness 275 m (Dusar & Houlleberghs, 1981).

The formation is expected to be present east of the fault as well. Locally, the sandstones are up to 300 m thick. There is however no information about the facies of the uppermost layers of the Coal Measures Group east of the Heerlerheide Fault. Based on the available information, it cannot be stated if a thick sandstone sequence is present and how thick it is. Further exploration is needed to verify the presence of the Neeroeteren Formation in the graben area and to characterize the reservoir properties of any late Upper Carboniferous sandstones.

Reservoir properties

The Neeroeteren Formation consists of quite homogeneous, medium to coarse-grained subarkosic to sublithic arenites (Bertier et al., 2006; Dupont, 1992). The porosity and permeability of the rock are reduced by the presence of authigenic quartz, clays (authigenic kaolinite and illite), and small

quantities of authigenic carbonates (dolomite/ankerite and siderite). Porosity is enhanced by dissolution of feldspars and by preservation of primary porosity due to the presence of grain-coating clays. Feldspar is predominantly altered to illite. However, as the influence of meteoric processes shortly after deposition was restricted, the amount of feldspar alteration was limited. More feldspar was preserved, and less clay minerals formed. This had a positive effect on the porosity and permeability of the sandstone (Bertier et al., 2006).

Porosities measured on core samples range from 11.5 to 26%, permeabilities from less than 0.1 mDarcy up to 2473 mDarcy (Bertier et al., 2008). Values above 1000 mDarcy have been measured in the coarse sandstones and conglomerates (Table 7). The average porosity measured on core samples is about 15%, average permeability 110 mDarcy.

Table 7: Porosity and permeability data of the Neeroeteren Formation from core analyses. A distinction is made according to grain size, based on core descriptions.

	Porosity (%)				Permeability (mDarcy)			
Lithology	**Max**	**Min**	**Av.**	**n**	**Max**	**Min**	**Av.**	**n**
Fine sandstone	26.0	6.5	13.1	41	10	0.1	2	35
Medium sandstone	19.8	5.0	15.1	50	315	d.l.	86	41
Coarse sandstone	30.0	3.5	16.8	61	1172	d.l.	172	44
Conglomerate	19.2	11.5	16.2	13	2473	14.3	336	10

Based on the core descriptions, the proportions of different lithologies were calculated (Table 8). Almost 29 % of the Neeroeteren Formation consists of fine-grained sandstone. 20 % is made up of medium-grained sandstone, 20 % of coarse-grained sandstone, 6 % of conglomerate. Siltstone makes up 17 % of the formation, mudstone almost 8 %, and coal layers nearly 2 %.

Table 8: Percentage of different lithologies within the Neeroeteren Formation, based on core descriptions from wells KB146, KB161, and KB172

borehole	**KB146**	**KB161**	**KB172**
Conglomerate	6	3	2
Coarse sandstone	20	31	17
Medium sandstone	19	30	41
Fine sandstone	29	27	33
Siltstone	17	2	6
Mudstone	8	4	1
Coal	2	3	0

The proportions of each lithology vary between the boreholes (Table 8). Boreholes KB161 and KB172 have around 90 % of sandstone, compared to less than 70 % for KB146. On the other hand, KB161 and KB172 contain less siltstone, mudstone, and coal. Another difference is the percentage of conglomerate, which is the highest in borehole KB146.

The permeability data suggest that the reservoir units within the Neeroeteren Formation correspond to the medium sandstones, coarse sandstones and conglomerate layers. They make up between 45 and 64% of the Neeroeteren Formation in the 3 wells shown in Table 8. The average net-over-gross ratio is 0.55.

Geothermal potential

Based on the core data, the Neeroeteren Formation is expected to be a productive geothermal reservoir in the northeast of Limburg. However, due to the lack of data about the thickness and reservoir properties of the sandstones over a large part of the study area, the Neeroeteren Formation is not included in this evaluation.

3.3.6 Geothermal potential of the Lower Carboniferous Limestone Group

Depth and thickness

In the study area the top of the Lower Carboniferous sequence is situated at a depth that ranges from -4800 on the 'Bree high' to -8300 m TAW in the Roer Valley Graben (Figure 4). According to the 3D model of Flanders, the thickness ranges from 425 m in the northeastern corner of the study area to 1080 m in the south. The quality of the seismic data in the area however does not allow accurate mapping of the thickness of the carbonate sequence. The true stratigraphic thickness of the Lower Carboniferous Limestone Group in MOL-GT-03 is 830 m including the transitional beds at the top and bottom of the sequence. The sequence of limestone and dolomite is 760 m thick. For the present evaluation, we assumed a minimal thickness of 450 m, an average thickness of 760 m and a maximal thickness of 950 m.

Reservoir properties

The reservoir quality of the Lower Carboniferous Limestone Group is largely defined by fractures and secondary porosity. The best way to define the reservoir quality is by well tests. Figure 12 shows the results of production and injection tests performed on the Lower Carboniferous lime- and dolostone in boreholes from the Campine area and Dutch Limburg. The data show a decline of the reservoir quality with depth. It also shows the heterogeneity of the reservoir. For example, the permeability of the limestone reservoir in the 3 boreholes drilled at the VITO geothermal plant span 3 orders of magnitude (Broothaers et al., 2021).

The large heterogeneity makes it difficult to predict the reservoir properties at any site. In general, one can assume that the Lower Carboniferous lime- and dolostones have moderate to excellent reservoir properties for geothermal up to about 2500 m. Below that depth, good reservoir conditions can be present in places with high secondary porosity, e.g., due to fracturing and/or dissolution.

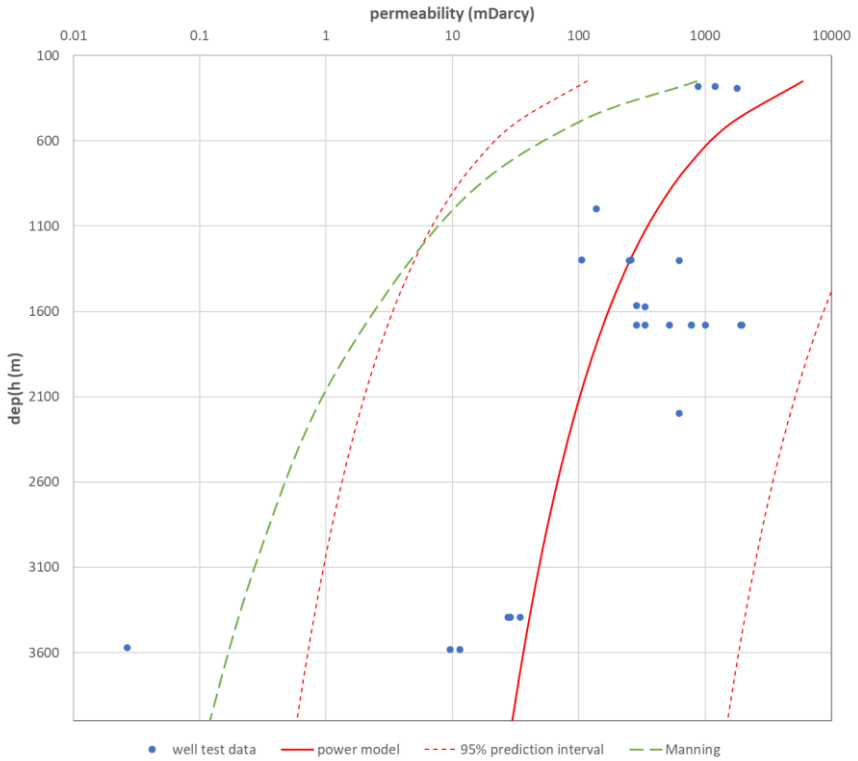

Figure 12: Change in permeability with depth for the Lower Carboniferous Limestone Group derived from production tests on boreholes from the Campine areas. The green dashed line shows the trend for deeply buried carbonates according to Ingebritsen & Manning, 1999.

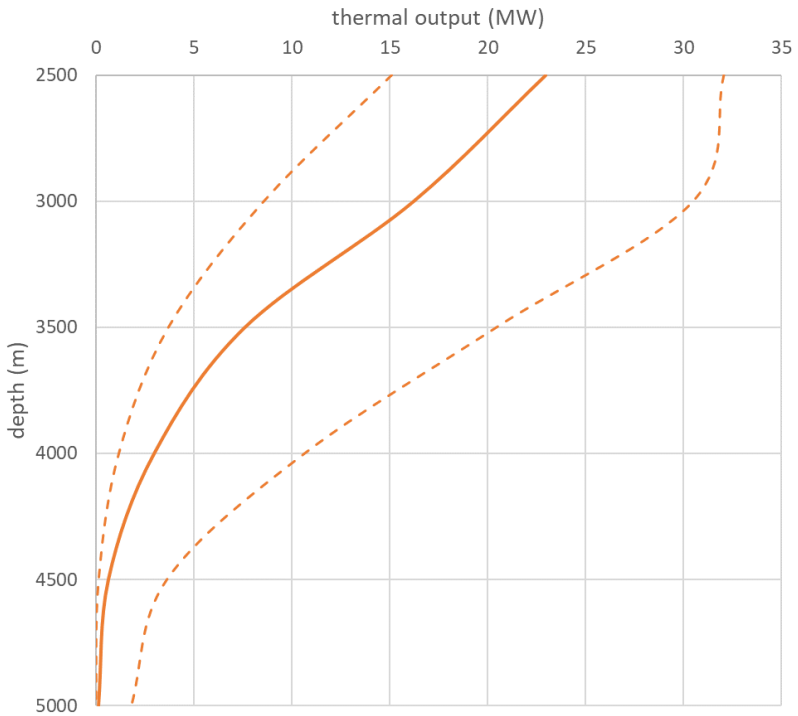

Figure 13: Calculated thermal output of a geothermal doublet targeting an area with average to high secondary porosity in the Lower Carboniferous Limestone Group. The solid line shows the p50 value calculated with DoubletCalc. The dashed lines show the p10 and p90 values.

Geothermal potential

Figure 13 shows the expected thermal output of a geothermal doublet that targets an area with average to high secondary permeability at a depth of 2500 to 5000 m. 'Average secondary permeability' refers to the value calculated from the power model shown in Figure 12. 'High secondary permeability' refers to the upper 95% confidence limit. For depths down to 3500 m there is a good chance that the geothermal doublet will have a thermal output of 4 MW or more. Below 4000 m, the p10 value of the predicted thermal output of drops below 10 MW. Based on these results and based on the current knowledge about the reservoir properties of the Lower Carboniferous Limestone Group, 3500 m is taken as the depth limit for geothermal projects targeting the lime- and dolostones.

The top of the Lower Carboniferous Limestone Group in the study area lays below the depth limit. For this reason, the limestones are not further considered as geothermal reservoir in this study.

3.4 Options for energy cascading in Bree

Based on the evaluation of the properties of the possible geothermal reservoirs, the most likely target in the study area are the Triassic sandstones. As the expected production temperature of a geothermal system targeting these sandstones is below the 65°C, the options for energy cascading are limited. Low temperature heating is an option, but for domestic district heating or other applications the temperature needs to be lifted using heat pumps. As the systems' efficiency goes down with the temperature lift that is needed, we restrict the current evaluation to the supply of heat for district heating and applications that need low temperature heat. The supply temperature of the heating grid was set at 65°C and the return temperature at 45°C.

The options for heat delivery and cascading were calculated from maps about geothermal potential and the heat demand in the study area using a spatial modelling tool that was developed by VITO in the context of the Flemish ERDF project 910: Geothermie 2020 (Vranckx et al., 2015).

3.5 Blueprint for geothermal district heating design in Bree

Figure 14 shows the general layout of the geothermal plant at Bree. The pressure difference that is needed to run the geothermal loop is generated by the production pump. Once the geothermal brine is at surface, it is passed through a particle filter to remove any sand or other fines that are released from the reservoir.

Next, the brine is used to heat-up water from the application loop. In case the temperature of the geothermal fluid is higher than the return temperature of the application (set at 45°C), the water is pre-heated using a first water-water heat exchanger. As in all possible cases, the temperature of the geothermal fluid is lower than the supply temperature needed by the application (set at 65°C), a heat pump is used to lift the temperature. A second heat exchanger is used to separate the heat pump from the geothermal fluid. The geothermal fluid is then sent to the injection well after having passed through another particle filter. At the application site, a storage tank is foreseen to stabilize the connection to/with the heating grid and the deal with short-term fluctuations in heat demand.

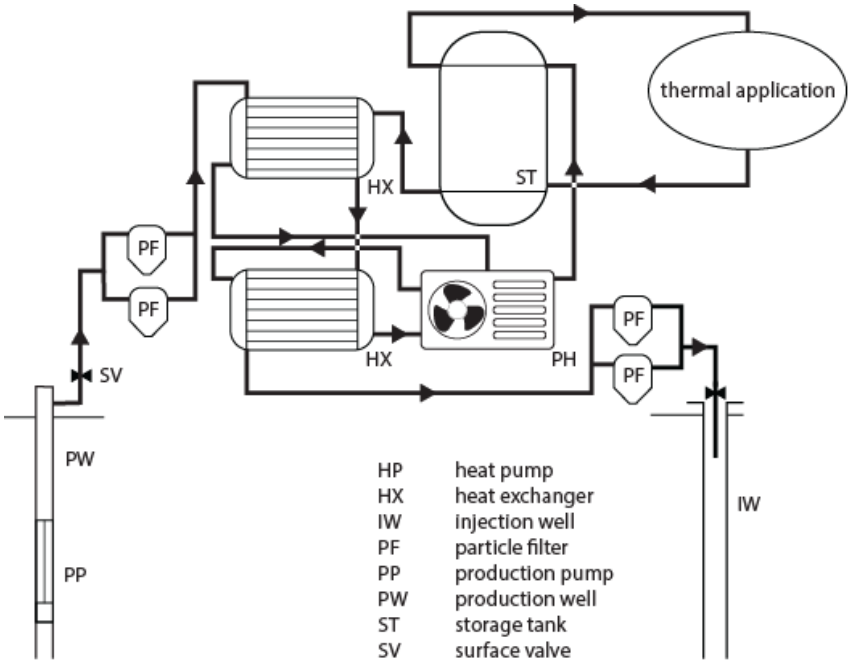

Figure 14: Schematic process chart of a low-temperature geothermal heating plant

3.6 Techno-economic feasibility of geothermal district heating in Bree

3.6.1 Preferred surface locations for geothermal plants

The preferred locations for geothermal plants were defined using the spatial optimization model developed by Vranckx et al. (2015). The approach is based on a spatially explicit calculation model that is based on the RuimteModel Vlaanderen (Het Ruimtemodel Vlaanderen | Ruimtemodel Vlaanderen), the heat map of Flanders (Warmtekaart | Vlaanderen.be) and the geological conditions discussed above. The model analyzes the profitability of geothermal energy for every possible underground location in the study area. It uses the following maps that supply input for the calculation:

- Suitability map: restrictive spatial preconditions provide an input map where geothermal energy is possible and desirable.
- Geothermal potential map.
- Heat demand map.
- Capex map: spatial distribution of the estimated investment cost for a geothermal plant based on the local geological conditions and the cost model discussed below.
- Opex map: spatial distribution of the estimated production cost of geothermal heat based on the local geological conditions and the cost model discussed below.

For each possible location, the model calculates the costs and benefits of supplying heat on an annual basis over the lifetime of a project. The project lifetime was set at 30 years. The result is primarily a map showing the profitability of a geothermal plant for all possible locations, given the set of input parameters.

The model connects clusters of heat consumers to the geothermal plant, not individual cells, to correctly estimate the costs of installing heat networks. For each location, the profitability per

MWh of heat supplied to each cluster is determined and the most profitable cluster is connected first. This process continues until all heat from a location has been sold to clusters.

As a next step, the model places the first geothermal plant in the most profitable location, if any. To prevent geothermal power plants from competing for underground heat, a minimum distance of 3 km is imposed. Around the first geothermal plant, the suitability is therefore reduced to 0 within a radius of 3 km. The heat demand map is also adjusted so that the clusters that are served by the geothermal plant are no longer available for additional geothermal plants.

Then a new profit map is calculated to place the next geothermal plant in the most profitable location in this profit map. These steps are repeated as long as there are profitable locations or until a maximum number of plants have been placed. In this way, an optimal placement of geothermal power plants is achieved.

The analysis is of course sensitive to the price of electricity and the sales price of the heat. The analysis is therefore carried out for different price levels. The spatial analysis is performed for both the current heat demand and the heat demand for future scenarios, based on the RuimteModel Vlaanderen.

3.6.2 Cost model

The cost model used to assess the options for geothermal energy cascading in Bree is based on the process chart sown in Figure 14. It includes the following items:

- Costs of geothermal exploration: this includes the costs for a 2D seismic survey assuming a cumulative length of the seismic lines of 60 km.
- Costs for field development: this includes the costs for site preparation and the drilling of two wells. The cost model for the drilling activities is based on an estimate of the materials used and the time needed for drilling and testing. The materials model was developed by VITO in the context of the study on "*Geothermal plants' and applications' emissions"* (Rocco et al., 2020). Prices for steel are based on the costs of carbon steel pipes and indexed using the carbon steel price index (base price 1,911.25 euro/ton, base index value 176.2). Costs for cement are derived from the price of fine ready-mix concrete and adjusted using the construction output price index (base price 175 euro/m^3, base index value 109.7). Other commodities included are fuel (1.2 euro/l), electricity (85 euro/MWh), mud (150 euro/m^3). Costs for these commodities are adjusted to the consumer price index (base index value 111.5). Besides, the model includes costs for the removal of cuttings and mud, costs for delivery and handling and day-rate costs. A rig day rate of 15.000 Euro was used for the current assessment.
- Costs for plant development: this included the capital costs for the components shown in Figure 14. The correlation given by Haslego & G. Polly (2002) was used to calculate the equipment capital cost for the plate and frame heat exchangers. The equipment capital cost for the storage tank and the particle filters were calculated from the correlations given by Smith (2005). The equipment capital cost for production and the heat pump were derived from equipment bought in the context of the Balmatt and DGE-ROLLOUT projects, and from quotations given by manufacturers. It was further assumed that all equipment that comes into contact with the geothermal fluid will be made from a high grade RVS (e.g., RVS321) and that operating pressure of the geothermal loop will be in the range of 10 – 20

bar. Finally, an installation factor of 1.5 was assumed to include costs for connections to the grid and/or piping.

All costs were recalculated to the year 2022 assuming a consumer price index of 123.05, a carbon steel index of 295.9 and a Chemical Engineering Plant Cost Index of 776.9.

3.6.3 Exploration cost

The exploration cost relates to the costs for a 2D seismic survey. The correlation is based on accrual costs for 2D seismic surveys conducted by VITO in Belgium and the Netherlands.

Equation 11:

$$EC_s = 134 + \mathrm{d}_t \times (2.15 + 1.4 * \mathrm{L}) + 5.6 * \mathrm{L}$$

With d_t the target depth in km and L the cumulative length of the seismic lines in km. Ec_s is given in kEuro for the year 2022 (CI = 123.05).

The cost of a 2D seismic survey of 60 km was included to calculate the investment map.

3.6.4 Drilling cost

To derive the map for the investment costs, a correlation was established between the drilling costs calculated for a set of preliminary well designs that cover the depth range of the Buntsandstein reservoir in the study area and drilled length. The cost includes supervision at a rate of 2500 Euro/day.

Equation 12:

$$DC = 2.05 \times 10^{-4} \times \mathrm{TD}^2 + 3.6 \times 10^{-2} \times \mathrm{TD} + 1290$$

With TD the well depth (TD). DC is given in kEuro for the year 2022 (CI = 123.05, csi = 295.9, copi = 126.4).

The costs for 2 identical wells are included to calculate the investment map.

3.6.5 Plant cost

To derive the map for the investment costs, a correlation was established between the plant costs estimated for a set of plant designs that cover the range in production temperature (temperature at the heat exchanger) and thermal output observed in the study area. The temperature range covered goes from 21 to 63°C. The thermal output ranges from 21 to 7100 kW.

Equation 13:

$$PC = -280 + 50.7 \times \mathrm{Q} + 16.50 \times T_{hx}$$

With Q the flow rate in kg/s and T_{hx} is the temperature at the heat exchanger (°C). PC is given in kEuro for the year 2022 (CI = 123.05).

T_{hx} is calculated as the estimated reservoir temperature minus the estimated temperature loss.

3.6.6 District heating costs

The costs for installing a heating network were calculated based on the distance between the geothermal plant and location of the heat demand. The distance is calculated as the crow flies. The cost was fixed at 1 MEUR per kilometer. In addition, a cost of 0,14 MEUR per ha was added to account for the connection of users to the heating network.

Heat loss was included as a constant decay of 3% per km.

3.6.7 Operating costs

The cost model used to assess the options for geothermal energy cascading in Bree includes the following items:

- Annual cost for electricity: this includes the energy needed to circulate the geothermal brine and the electricity needs for the heat pump. As the estimated production temperature over the entire study area is estimated to be below 65°C, a heat pump is needed to deliver heat for domestic purposes.
- Annual maintenance costs for the wells: well maintenance is set at 2.5% of the drilling cost.
- Annual maintenance of the geothermal plant: plant maintenance is set at 2.5% of the investment cost.

The annual cost for electricity is calculated as:

Equation 14:

$$OC_{elec} = \frac{HC \times load \times c_{elec}}{COP_{system}}$$

With HC the thermal capacity of the geothermal plant in MW, load the load factor (set at 0.6) c_{elec} the electricity price (set at 85 Euro/MWh) and COP_{system} the COP of the geothermal plant. The COP of the geothermal plant is calculated from the COP of the geothermal loop (COP_{wells}) and the COP of the heat pump (COP_{HP}):

Equation 15:

$$COP_{system} = \frac{COP_{wells} \times COP_{HP}}{COP_{wells} + COP_{HP}}$$

COP_{wells} was calculated using DoubletCalc for 17 potential cases that span the variability of the reservoir properties of the Buntsandstein in the study area. The average COP_{wells} for the 17 cases is 23.3, with most values between 15 and 25.

COP_{HP} was derived from a thermodynamic model for a heat pump with ammonia as working fluid using the thermodynamic database REFROP (Lemmon et al., 2018). It was assumed that the brine is cooled by 10°C over the second heat exchanger. Assuming a pinch temperature of 2°C, the

injection temperature varies therefore between 37°C and 9.6°C for the 17 cases studied. The average injection temperature is 29.1°C.

3.7 Results of the spatial optimization model

Figure 15 and Figure 16 show results of the techno-economic spatial optimization for Bree using two different assumptions for the heat prices: a low scenario with a heat price of 40 Euro/MWh and a high scenario with a heat price of 100 Euro/MWh.

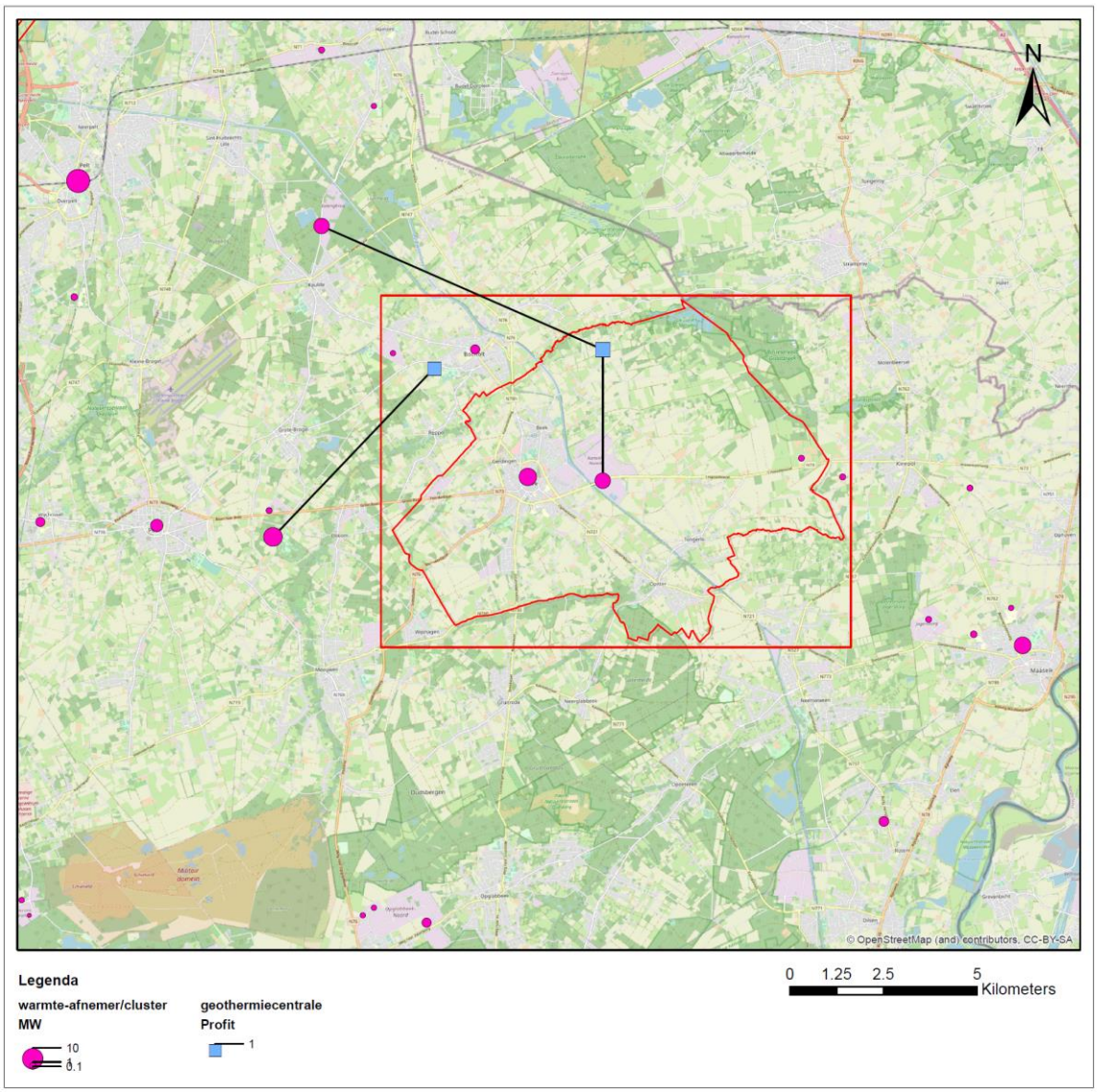

Figure 15: Result of the techno-economical optimization for locating profitable geothermal plants in the Bree area based on a heat price of 40 Euro/MWh

In the low scenario, the optimization tool finds 2 profitable locations for a geothermal plant. The first plant supplies heat from the northern part of the area to users at the industrial area of Kanaal-Noord and a few industrial users north of Bocholt. The second geothermal plant is connected to the holiday park Erperheide in Peer. The cost to cover the large distance between the geothermal plants and the users is compensated by the large heat demand of the connected users.

In the scenario with a heating price of 100 Euro/MWh, the tool finds 6 locations for profitable geothermal plants. Most of the geothermal plants are connected to one or a few industrial users with a high to moderate heat demand (> 1,000 MWh/year). In addition, cases for geothermal district heating appear in the centers of Bree, Bocholt and Meeuwen.

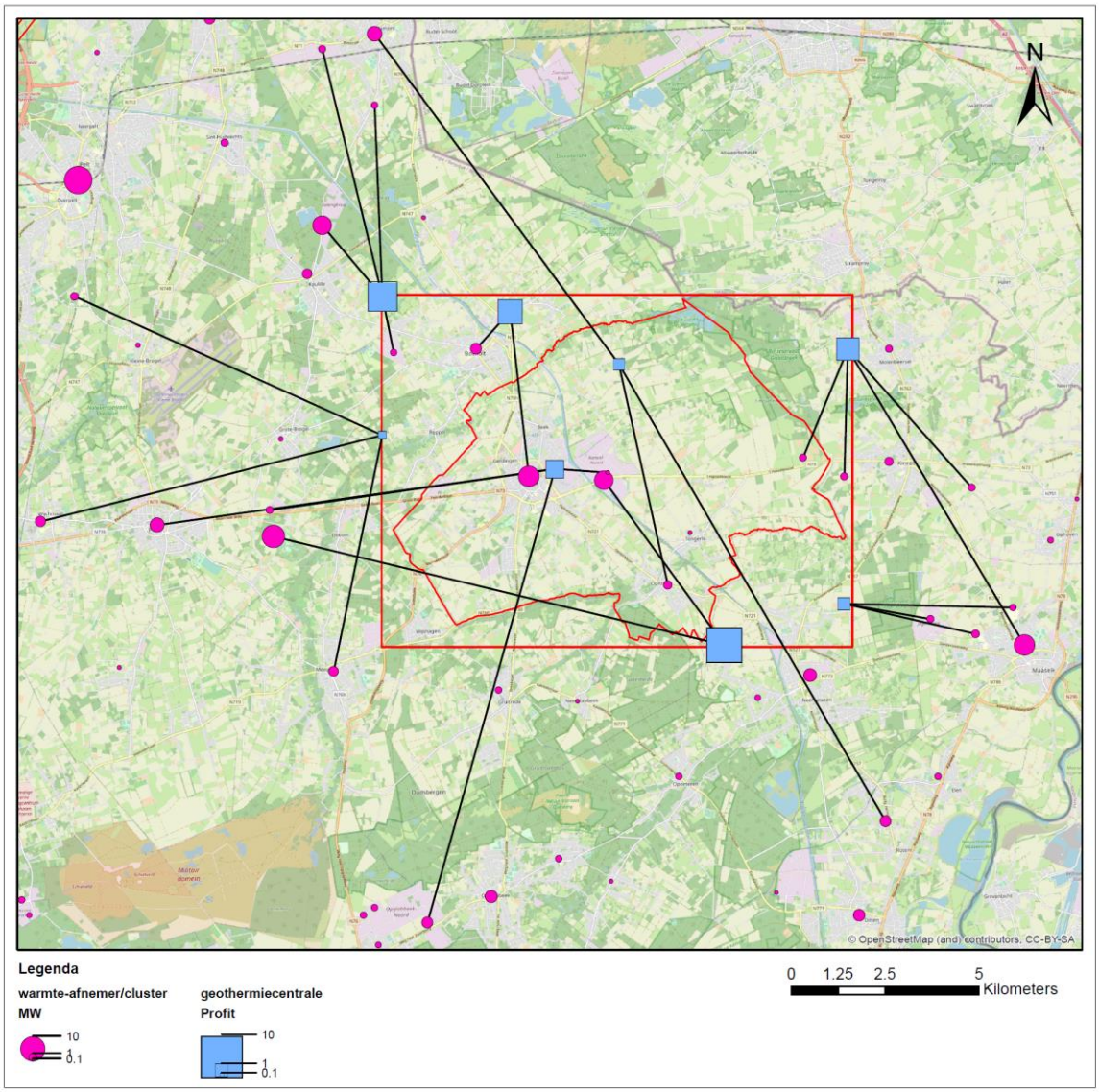

Figure 16: Result of the techno-economical optimization for locating profitable geothermal plants in the Bree area based on a heat price of 100 Euro/MWh

4. Techno-economic feasibility of geothermal district heating in Lommel

4.1 Objectives

The objective of this exercise is to evaluate whether there are locations within the municipality of Lommel (province of Limburg, Belgium) that may be suitable for the development of deep geothermal district heating. It is a first step in the evaluation of the techno and socio-economic viability of potential geothermal projects in Lommel.

4.2 Area of interest

The area that is screened for possible locations for geothermal district heating coincides with the territory of the municipality of Lommel. The study area covers 102.28 km^2 (Figure 17). Lommel has about 34,000 inhabitants. Most of the population lives in and near the city of Lommel. Lommel is the third largest shopping city in Limburg with a commercial and shopping center.

Lommel has several industrial areas and is one of the strongest economic growers in Flanders. The city continues to strengthen its economic position with the development of 276 hectares of new business grounds at Kristalpark. This industrial area is located southwest of the city center. Lommel also hosts one of the three Belgian Center Parcs holiday parks: Vossemeren. The holiday park, including a subtropical swimming pool, is located north of the city center, between the canal Herentals – Bocholt and the Dutch border.

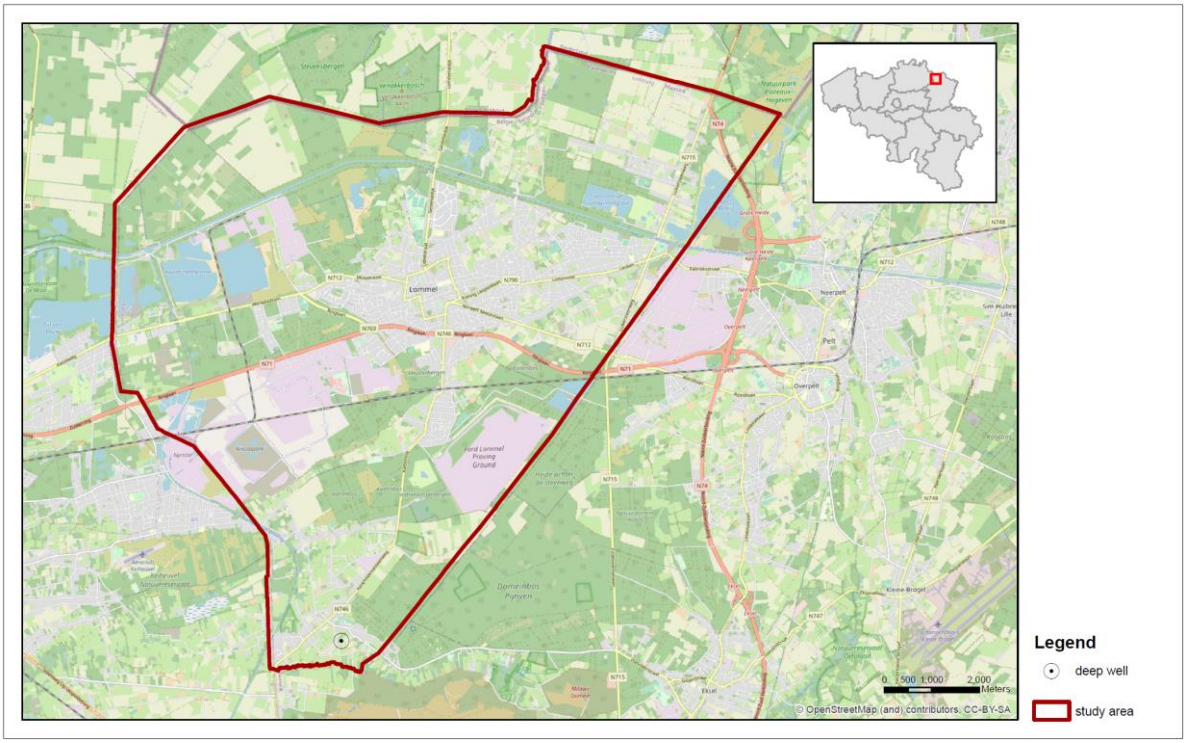

Figure 17: Map of the area that is screened for possible locations for geothermal district in Lommel showing may locations of habitation and industrial activity

4.3 Geological conditions

4.3.1 Used data

Wells

Table 9Table 1 gives an overview of the wells that were used in the evaluation. Only well 047W0264 - Lommel-Kerkhoven lies inside the study area. The well was drilled for coal exploration and reaches a depth of 1504 m. Information about the lithostratigraphy and characteristics of deeper geological strata was derived from wells outside the study area. The data was extrapolated based on observed depth trends and 3D Geological Model of Flanders (Geologisch 3D-model G3Dv3 | DOV (vlaanderen.be)). The depth trends used for the extrapolations are discussed below.

Stratigraphic information and data from the wells was derived from the Databank Ondergrond Vlaanderen | DOV, the NLog Datacenter and an in-house database of VITO.

Id	Well	X (m)	Y (m)	Z (m TAW)	Total depth (m)
031E0161	Mol	205351	212539	29.0	-
031W0387	Dessel Fish	198625	213475	24.0	699.84
047E0196	Hechtel-Hoef	220097	199325	69.0	1500.2
047W0251	Leopoldsburg	214050	200880	57.8	1754.1
047W0264	Lommel-Kerkhoven	213940	206368	46.0	1504
MOL-GT-1	MOL-GT-01-(S1)	201783	212961	25.0	3610
MOL-GT-2	MOL-GT-02	201791	212962	25.0	3715.15
MOL-GT-3	MOL-GT-03(-S1)	201768	212960	25.0	4234.61
046E0281	Heppen	209526	200550	46.0	1312.5

Table 9: Wells used to locate potential sites for geothermal district heating in Bree. Coordinates are in Lambert 1972.

Datasets

Next to the wells shown in Table 9, the following datasets were consulted:

- '*Compilatie en Duiding van Warmtedata in de Diepe Ondergrond van Vlaanderen en Opmaak van een Warmtefluxkaart*': A compilation of temperature data of the Flemish subsurface commissioned by the Flemish Planning Office for the Environment (VPO)
- DOV Verkenner (vlaanderen.be): Lithological data and data from cores/cuttings available through the database of the Flemish Subsurface.
- Reservoireigenschappen | NLOG: A dataset of historical and more recent quantitative estimates of reservoir properties of lithostratigraphic units in the Dutch deep subsurface based on borehole measurements and cores prepared by TNO.

- NLog_poroperm.xlsx (Boringen | NLOG): A dataset of petrophysical measurements on cores from deep wells created by TNO.

Geological models

Depth and thickness maps were adopted or calculated from the 3D Geological Model of Flanders (Geologisch 3D-model G3Dv3 | DOV (vlaanderen.be))

The temperature model was adopted from the compilation of temperature data of the Flemish subsurface and the heat flux map of Flanders (Broothaers et al., 2020)

4.3.2 Methodology

General approach

The methodology used to estimate the geothermal potential in the study area is the same as the one used for Bree. According to previous inventories, 3 stratigraphic intervals qualify as potential reservoirs in the area (Berckmans and Vandenberghe, 1998):

- Chalk Group: the porous carbonate rocks of the Maastricht and Houthem formations of Late Cretaceous and Early Palaeocene age;
- German Trias Group: sandstone layers within the Röt and Buntsandstein formations of early Middle to Early Triassic age;
- Lower Carboniferous Limestone Group: fractured and locally karstified carbonate rocks of Visean to Tournaisian age.

The present evaluation focusses on the sandstones of the German Trias Group and the carbonate rocks of the Lower Carboniferous Limestone Group. Based on the sub-crop map of the Carboniferous and Devonian formations in the Campine area (Langenaeker, 2000), the Neeroeteren sandstones are not expected to occur in the western and central part of the study area. They may be present in the northeastern part.

The chalks of the Maastricht and Houthem formations were not included in the analysis as the expected formation temperature is too low for deep geothermal district heating.

4.3.3 Subsurface model DGE aquifers Lommel

Lithostratigraphy

The Quaternary and Tertiary sequence mainly consists of coarse to fine grained siliciclastic sediments. An overview of the Quaternary and Tertiary sequence in the study area is given in Deckers et al. (2014). The succession consists of (Figure 1):

- Ghent Formation: aeolian sands of Quaternary age;
- Sterksel Formation: coarse sands and gravel of Quaternary age;
- Mol Formation: medium to coarse, white sands with lignite, deposited during the Late Miocene to Pliocene and possibly even Quaternary;
- Kasterlee Formation: fine to medium glauconitic sands of Late Miocene age;
- Diest Formation (Late Miocene): glauconitic sands;

- Berchem and Voort Formation (Middle Miocene to Late Oligocene): medium to fine sands with glauconite and shell fragments;
- Eigenbilzen Formation (Oligocene): dark green, glauconite rich, clayey, fine-grained to medium-grained sands, with bioturbations;
- Boom Formation (Oligocene): alternating bands of clay and silt with septaria;
- Bilzen Formation (Early Oligocene): sands (the Kerniel Member and the Berg Member) with a clayey intercalation (the Kleine-Spouwen Member);
- Sint-Huibrechts-Herne Formation (Early Oligocene): fine, clayey sand with glauconite and shell fragments;
- Lede Formation (Middle Eocene): calcareous and glauconiferous, fine sand, with a few sandy limestone or calcareous sandstone layers;
- Tielt and Hyon Formation (Early Eocene): very fine, clay-rich sand and silt;
- Kortrijk Formation (Early Eocene): clay with intervals of silt to fine sand containing glauconite;
- Mons-en-Pévèle Formation: very fine clay-rich sand containing glauconite. Although the Formation status is given to the Mons-en-Pévèle sand unit , arguments could be forwarded to consider it as a Member of the Kortrijk Formation.
- Hannut Formation (Late Paleocene): marly clay, clay to sand at the top and local incision by continental clays and sands of the Tienen Formation. The Eocene represents a hiatus due to erosion during the last Eocene. That erosion also cut into the Hannut Formation, which is therefore locally thin.
- Heers Formation (Middle Paleocene): glauconitic sand and marl;
- Houthem Formation (Early Paleocene): calcarenites

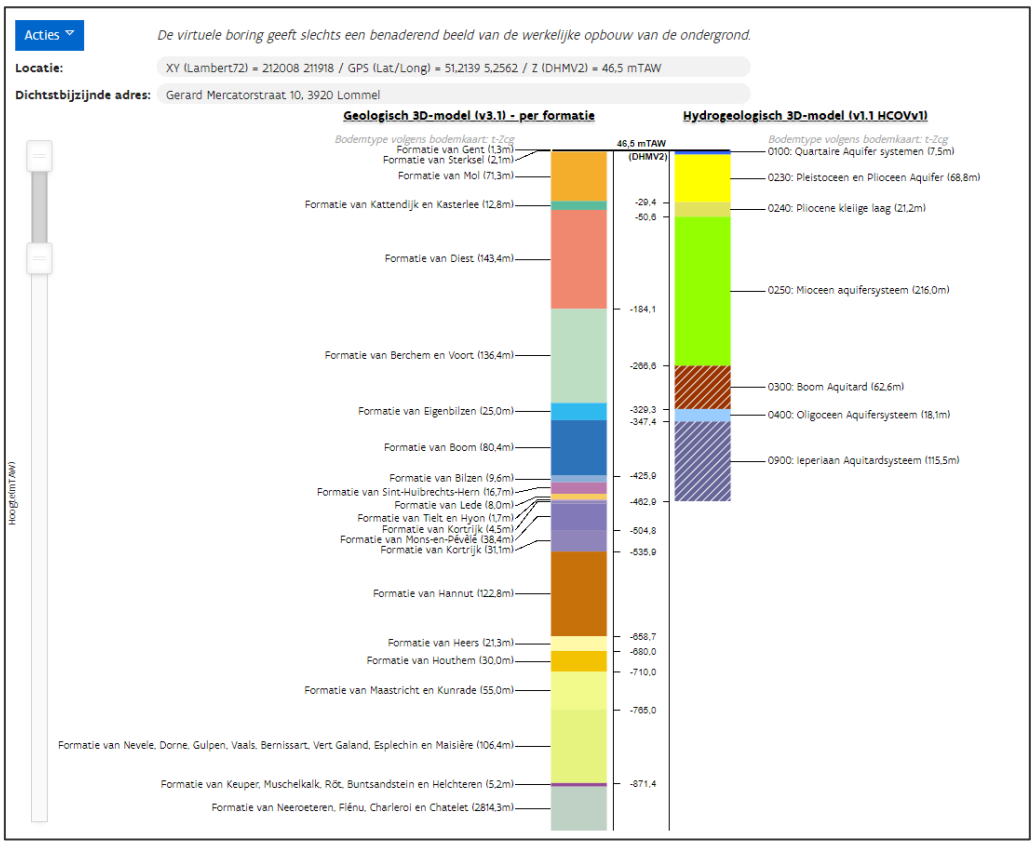

Figure 18: Post-Carboniferous lithostratigraphy and hydrogeology at the Kristalpark industrial area (Virtuele boring (vlaanderen.be))

Chalk Group

The Chalk Group is mainly made up of carbonate rocks. The majority consists of white, pale yellow, cream and light grey, hard, fine-grained bioclastic limestones and marly limestones. The Chalk Group dips towards the north – northeast. In the southern part of the study area, the top is situated at a depth of -550 – -600 m TAW (Figure 19). In the north a depth of -960 m TAW is reached. The sequence is transected by northwest – southeast trending normal faults Throws along the faults are of the order of 40 m or less.

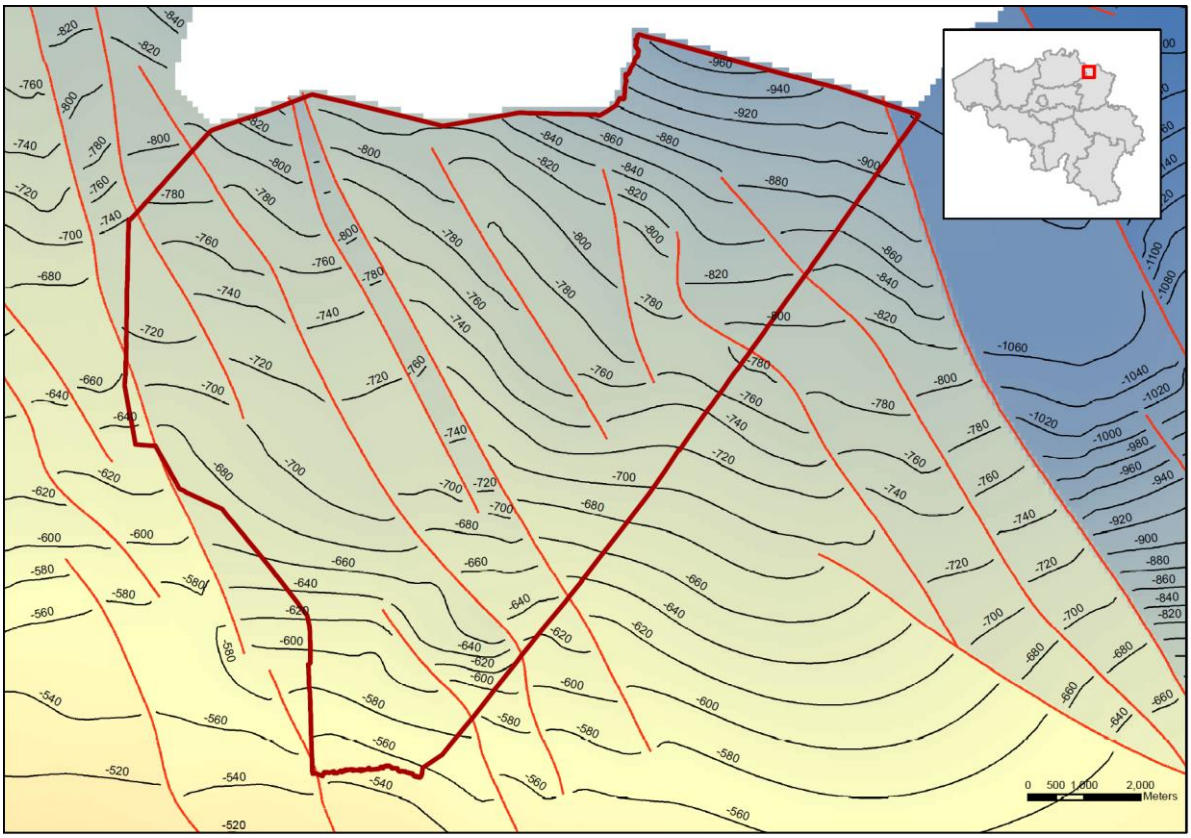

Figure 19: Map of the depth of the top of the Cretaceous (G3D v3.0)

Altena Group

In the northeastern corner of the study area, deposits of the Late-Triassic to Jurassic Altena Group are preserved. The sequence predominantly consists of marine claystones, with sandy and calcareous intercalations (Dusar et al., 2001; Laenen, 2002). In the study area, deposits of the Sleen Formation are expected. They consist of grey, fossiliferous claystone. The top is formed by a brown, locally sandy claystone, often rich in megaspores.

German Trias Group

Mostly red to variegated siliciclastic sediments, locally rich in anhydrite. The upper part is rich in marl, limestone and dolomite layers. The lower part consists mainly of sand- and siltstones with conglomerate levels. The German Trias Group is of early Middle to Early Triassic age.

- Keuper Formation: an alternation of red-green claystone and clay-rich dolomite to dolomitic marls. The base is sandy and often psammitic. The presence of anhydrite and gypsum layers or nodules is characteristic.
- Muschelkalk Formation: a sequence of grey to mottled marls, clay-rich dolomites and limestones, anhydritic claystones and anhydrite layers.
- Röt Formation: in the Campine area, the Röt Formation consists of an alternation of reddish brown to greenish, silty and anhydrite rich claystone, and anhydrite. The basal part consists of an alternation of psammitic sand and claystone with thin anhydrite layers. The boundary with the underlying Buntsandstein Formation is difficult to draw due to absence of massive evaporite layers.
- Buntsandstein Formation: a sequence of reddish brown, sometimes mottled siliciclastic deposits ranging from claystone to conglomerate. Locally, the lithology is calcareous. The Buntsandstein is distinguished from the Röt Formation by the scarcity or absence of evaporites and a sandier character.

Helchteren Formation

The Helchteren Formation of Permian age consists of grey, marly sediments and grey, often nodular, clay-rich limestone beds. A red conglomerate layer is often found at the top.

Belgian Coal Measures Group

The Belgian Coal Measures mainly consists of carbonaceous, siliciclastic deposits of Westphalian and Namurian age. The facies evolves from open marine at the base over lower and an upper delta plain to alluvial at the top. In the study are, the group is subdivided in 6 formations:

- Neeroeteren Formation: predominantly consists of pale, massive, partly coarse-grained to conglomeratic sandstones. The pale color is a result of feldspar weathering and the formation of kaolinite. The sandstones show high porosity and permeability. They are interspersed with brightly colored siltstones and a rare coal seam. The siltstones become more numerous towards the top. The top is eroded everywhere.
- Flénu Formation: consists of a rhythmic sequence of coal, siltstones and sandstones. It contains more coal seams than the underlying Charleroi Formation and the coal seams are generally thicker. Subdivision of the Flénu Formation is possible based on volcanic ash layers and some weak, marine incursions.
- Charleroi Formation: is characterized by a rhythmic succession of coal, siltstones and sandstones. The coal seams are more numerous and thicker than in the underlying Châtelet Formation. The Charleroi Formation can be divided based on the presence of (weak) marine incursions.
- Châtelet Formation: consists of non-marine claystones, siltstones and sandstones in which thin coal layers and root beds occur sporadically. Notwithstanding the low coal content, mineable coal seams are present. The formation can be subdivided based on the presence of goniatite-containing marine layers.

- Andenne Formation: largely consists of a cyclical succession of non-marine, silty claystones and sandstones with thin coal seams and root beds. Thin marine claystone beds with goniatites are found as well as limestone beds. Thick (up to 30 m), bleached, quartzite sandstone bodies occur at different stratigraphic levels.
- Chokier Formation consists of calcareous claystones and bituminous claystone rich in pyrite (ampelite) and silicate rocks. It contains a rich marine fauna (including goniatites and Posidoniellae).

Lower Carboniferous Limestone Group

The Lower Carboniferous Limestone Group mainly consists of dark grey, grey to beige, limestones and/or dolomites. Locally calcareous clay or sandstone levels occur. The limestones and dolomites are locally karstified. In many places the top is silicified. Chert occurs at certain stratigraphic levels. In the north of Limburg, there are no deep wells that reach the limestones. Therefore, the actual nature of the deposits in the area can only be deduced from wells in Dutch Limburg and trends observed along the southern border of the Campine Basin. It is expected that the top of the limestones in the study area consists of thin to thick banked, grey to black limestones and dolomites of the Goeree Formation. Towards the top, the formation becomes clay-rich with the appearance of carbonate-rich or silicified black claystones that grade gradually into the black claystones of the Souvré Formation. The base of the sequence is expected to consist of an alternation of dark grey, partly calcareous claystones, nodular claystones, limestones and grey, sometimes micaceous silt and sandstones that belong to the Bosscheveld Formation. A detailed description of the lithostratigraphy of the Lower Carboniferous Limestone Group in the Campine area is given in Laenen (2003).

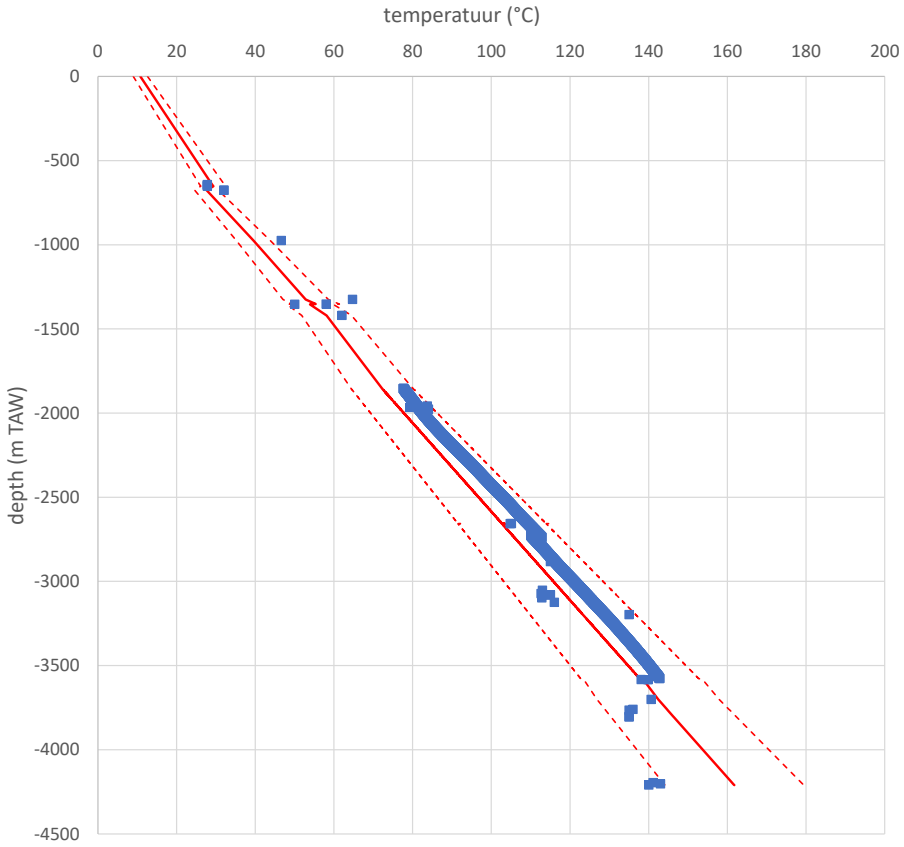

Figure 20: Temperature data and estimated subsurface temperature for Lommel with 95% prediction interval

Temperature model

Broothaers et al. (2020) show that temperature in the uppermost 50 m of the subsurface is constant at 11.0 ± 1.8°C. When discarding measurements made above 0 m TAW, the temperature data reveals a clear linear trend with depth starting at a temperature of 10.8 ± 1.8°C at 0 m TAW. Based on these observations, the following temperature model is defined for the study area:

Equation 16 (for the post-Cretaceous sediments):

$$T_z = 11 - 0.022 \times z$$

Equation 17 (for a depth below the top of the Cretaceous):

$$T_z = 11 + 0.015 \times z_{tC} - 0.038 \times z$$

With T_z the temperature at depth z in °C, z_{tc} the depth of the top of the Cretaceous and *z* the depth in meter relative to TAW (negative values are below 0 m TAW).

The model is based on bottom hole temperatures (BHT) measured in wells from the area (Table 9; Figure 20). The temperature log data and BHT readings are not corrected. Most of the measurements were made shortly after (the section of) the well had been drilled. Moreover, the model is constrained till a depth of 4000 m.

Potential geothermal reservoirs units

- Buntsandstein Formation

Vandenberghe (1991) identified the Buntsandstein Formation as a potential geothermal target. In the Campine area, the Buntsandstein is divided in 3 members:

- Bree Member: The upper part consists of red to mottled, fine to medium sandstones. Thin gypsum and anhydrite layers may occur near the top, as well as numerous gypsum or anhydrite nodules and gypsum or anhydrite filled veins. The lower part is characterized by an alternation of shale and sandstone. The color is predominantly red, sometimes mottled or bleached. The sandstones are very fine to medium fine and often calcareous.
- Bullen Member: A monotonous sequence of red to mottled, medium to very coarse sandstones and conglomerates. Locally, fine sandstones and siltstones, as well as calcareous levels occur.
- Gruitrode Member: Red to reddish brown sand- to siltstones. The upper part of the member consists of sand- and siltstones. The sandstone beds range from very fine to very coarse. Locally, conglomerate layers occur. The lower part of the member consists of siltstones with calcareous nodules and fine sandstone intercalations. Near the top of the lower unit paleosols occur.

The Bullen Member and the upper, sandy part of the Gruitrode Member are an equivalent of the Dutch Nederweert Sandstone Formation (Nederweert Sandstone Formation | DINOloket). The sandstones of the Buntsandstein Formation have been marked as potential geothermal reservoirs in the northeastern part of Limburg as well as in Dutch Limburg and Noord-Brabant (Milius, 1983; Vandenberghe, 1991; Berckmans & Vandenberghe, 1998). Based on the succession found in wells in and near the study area, two reservoir levels can be identified: the sandstones of the Bree Member and the sandstones of the Bullen Member and the upper part of the Gruitrode Member (Nederweert Sandstone).

The top of the Buntsandstein Formation is situated at a depth of -800 to -1000 m TAW (Figure 21). The top of the formation dips towards the north. This trend is transected by normal faults with throws up to about 60 m.

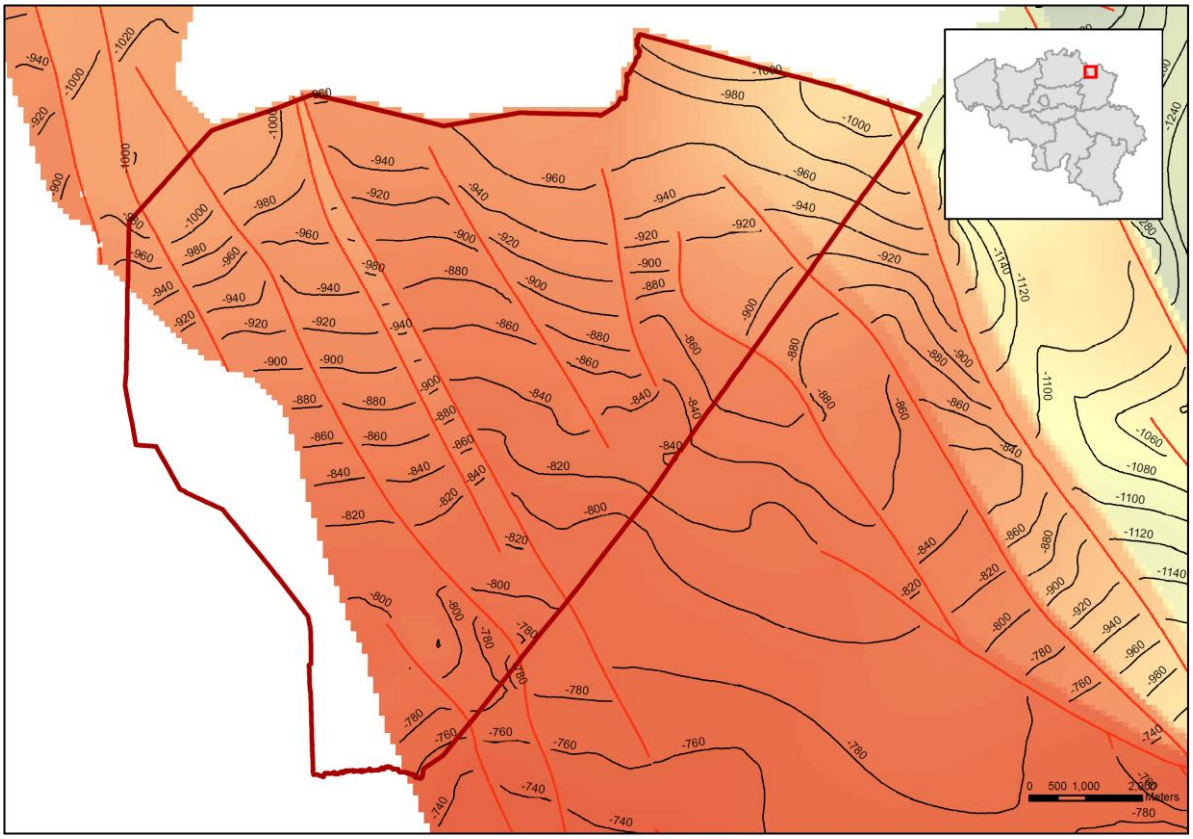

Figure 21: Map of the depth of the top of the Buntsandstein Formation (based on G3D v3.0)

- Lower Carboniferous Limestone Group

The karstified and fissured limestones and dolomites of the Carboniferous Limestone Group are marked as a regional geothermal reservoir in the Campine area (Vandenberghe, 1991; Berckmans & Vandenberghe, 1998; Broothaers et al., 2021). The Lower Carboniferous Limestone Group however has not been drilled in the study area. The geothermal potential of the sequence hence can only be deduced by extrapolation of data from wells that were drilled in the western part of the Campine area.

In the study area the top of the Lower Carboniferous sequence is situated at a depth that ranges from -4000 in the south to over -6000 m TAW in the north (Figure 22). Along the western border of the study area, the geological model suggests a major fault zone with a throw of several hundred meters, and resulting in an abrupt deepening of the Lower Carboniferous east of it.

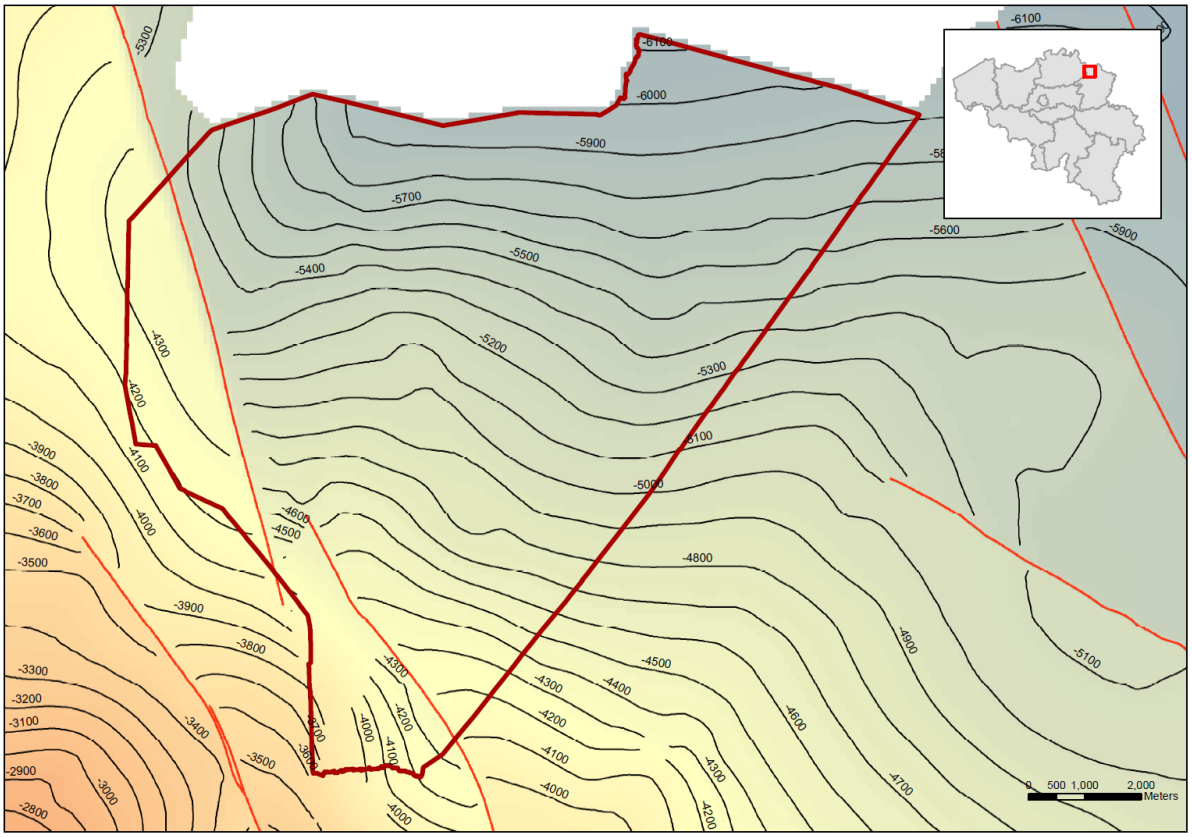

Figure 22: Map of the depth of the top of the Lower Carboniferous (G3D v3.0)

4.3.4 Geothermal potential of the Buntsandstein Formation

Depth and thickness

In the study area the top of the Bundsandstein Formation is located at -800 to -1000 m TAW (Figure 21). In the wells that penetrated the Buntsandstein in the Campine area, the thickness ranges from 1 to 566 m (Table 4). The maximal thickness of the Bree Member is about 190 m. The maximal thickness of the Bullen Member varies between 210 and 230 m. The thickness of the Gruitrode Member varies more: from 38 m in well 063W200 to 94 m in well 047E196. The member becomes thicker towards the northwest. The combined thickness of the Bullen Member and the sandy upper part of the Gruitrode Member (Nederweert equivalent) can reach up to 285 m.

The Triassic sandstone wedge out towards the west due to erosion. Based on the G3Dv3 model, the thickness of the Bree Member increases from 0 m 190 m in the east (Figure 23). In the western and central part of the study area, a large part of the Bree Member has been eroded. In the east, the entire member is preserved and younger sediments of Triassic to Jurassic age are present.

Along the western border of the study area, the thickness of the Nederweert equivalent quickly increases from 0 to more than 250 m (Figure 24). This trend is due to erosion of the entire Triassic sequence in the westernmost part of the study area. In the central and eastern part, the entire sequence is preserved. Here the sandstones that belong to the Nederweert equivalent can be up to 285 m thick.

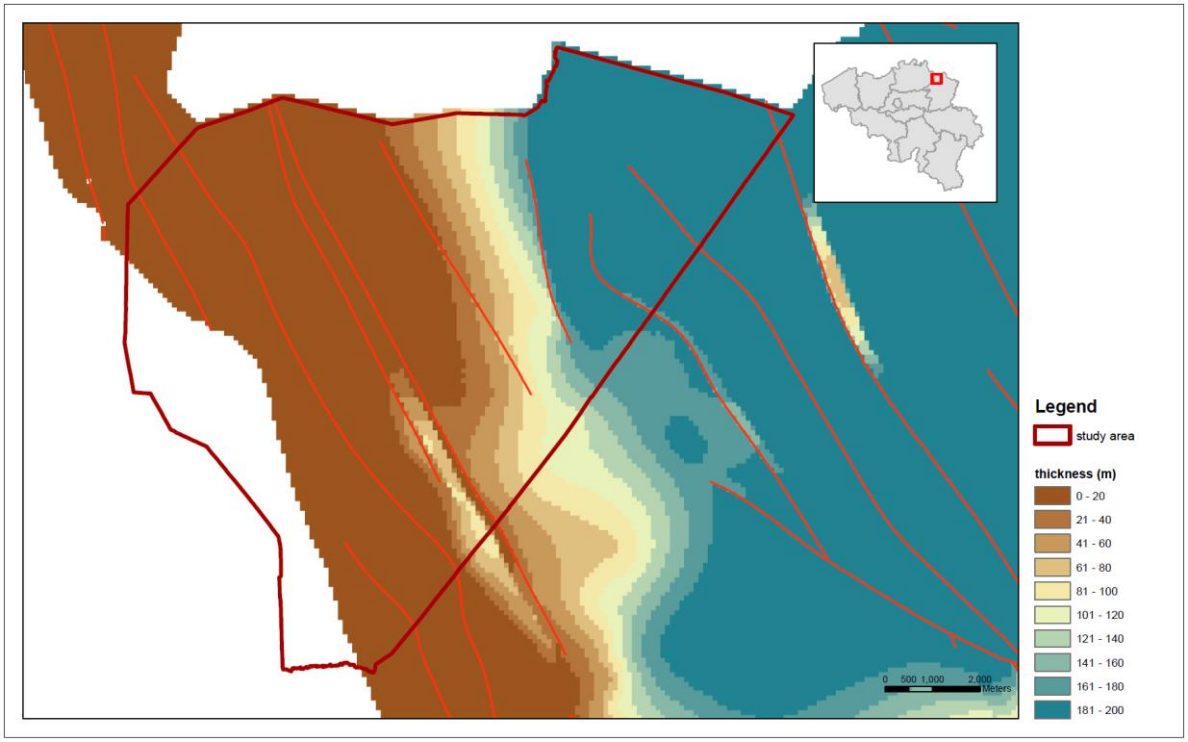

Figure 23: Thickness of the Bree Member in the Lommel area

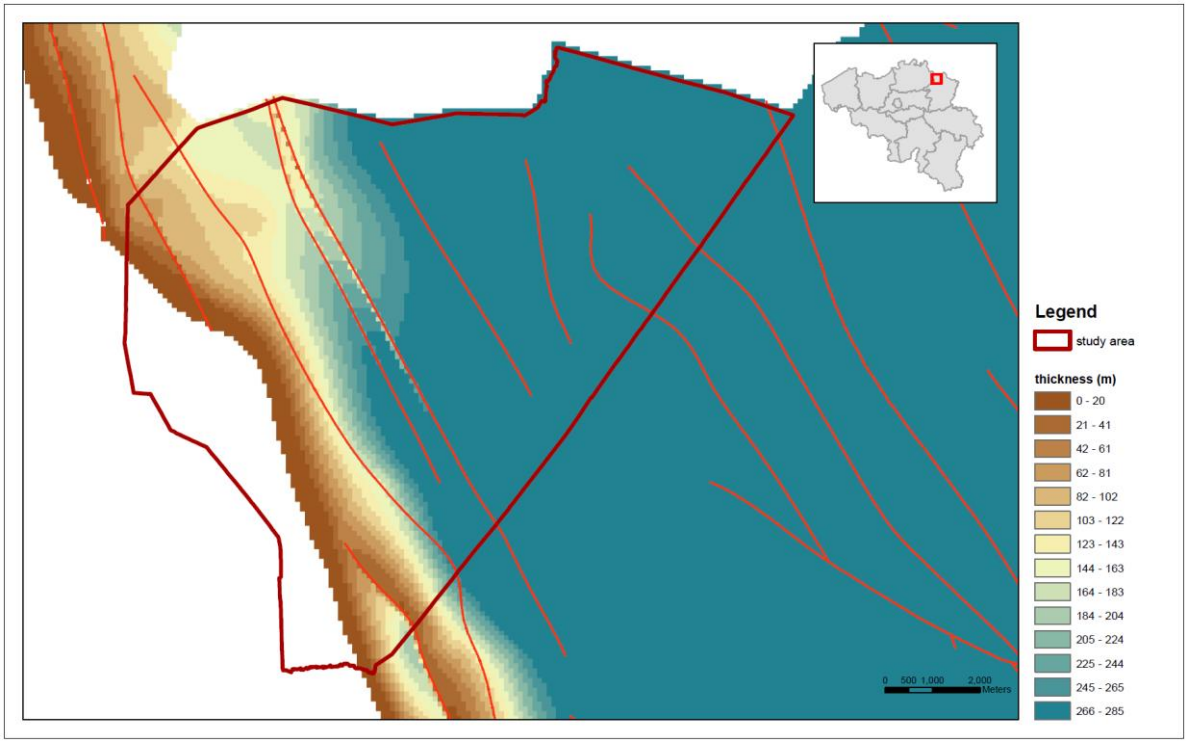

Figure 24: Thickness of the Bullen Member and sandy part of the Gruitrode Member (Nederweert equivalent) in the Lommel area

Reservoir properties

A discussion of the reservoir properties of the Bree Member and the Nederweert equivalent is given in the corresponding section for the Bree case.

Geothermal potential

The geothermal potential of the Bullen Member and from the Nederweert equivalent was calculated using the correlations given in the section Methodology (Table 2). The validity of the correlations was tested by comparison with the geothermal output calculated using DoubletCalc v1.4.3. at 8 locations in the study area. The R^2 of the correlation is 0.998. The correlation has a slope of 1.00 and an intercept of 0.02. It is concluded that the correlations can be used for a first assessment of the geothermal potential for the Bree Member and the Nederweert equivalent.

Equation 18:

$$\Delta P = 2 \times P_{res} \times 0.1$$

With P_{res} the hydrostatic pressure at the top of the reservoir.

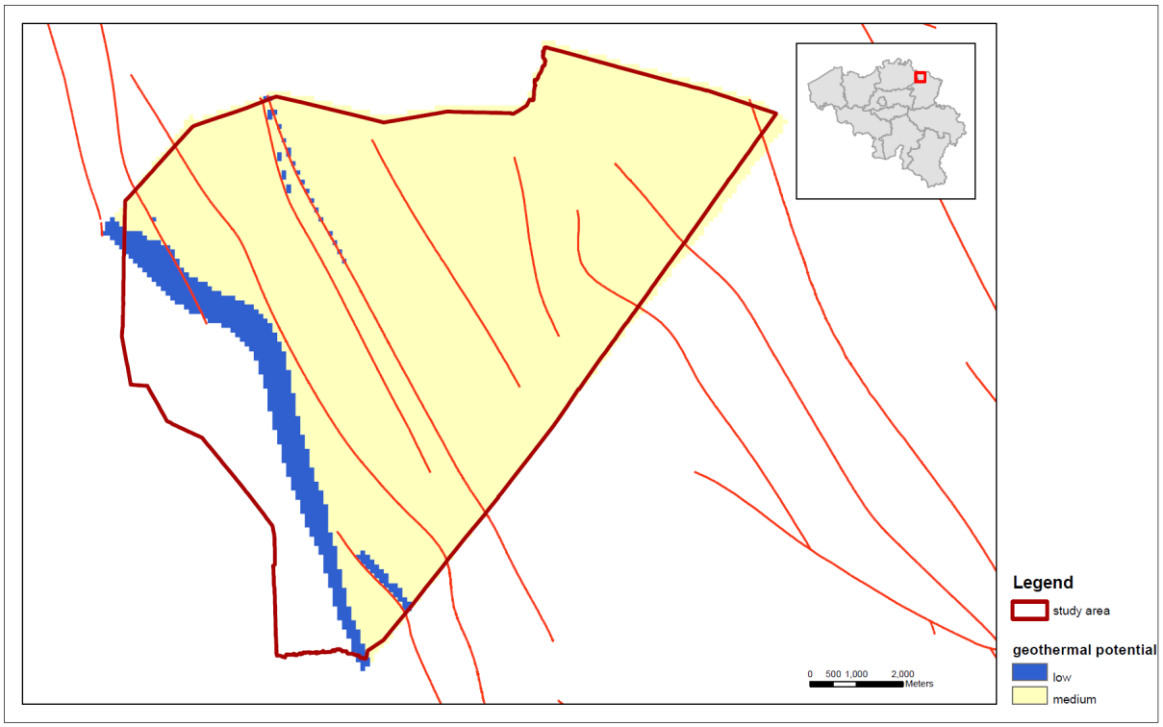

Figure 25: Map of the geothermal potential of the Buntsandstein Formation in the Lommel area based on the criteria discussed in the section methodology of chapter 3.

The total geothermal potential of the Triassic sandstones was calculated as the average potential of the Bree Member and Nederweert equivalent (Figure 25). Over most of the study area, the geothermal potential is moderate. The moderate potential is due to the low production temperature: a high potential is only assigned in case the production temperature is 65°C or more.

Over most of the study area, the transmissivity of the Triassic sandstones is moderate to high. This should allow flow rates of 24 kg/s or more. Along the western border, the potential is low as most of the sandstones are eroded.

Maps showing the estimated production flow rate for the two stratigraphic sub-units are given in Annex 1. The estimated formation temperatures are show in Annex 2.

4.3.5 Geothermal potential of the Lower Carboniferous Limestone Group

Depth and thickness

In the study area the top of the Lower Carboniferous sequence is situated around -4000 in the south to over -6000 m TAW in the north (Figure 22). According to the 3D model of Flanders, the thickness ranges from 760 m in the northeastern corner of the study area to 1100 m in the south-west. The quality of the seismic data in the area however does not allow accurate mapping of the thickness of the carbonate sequence. The true stratigraphic thickness of the Lower Carboniferous Limestone Group in MOL-GT-03 is 830 m including the transitional beds at the top and bottom of the sequence. The sequence of limestone and dolomite is 760 m thick. For the present evaluation, we assumed a minimal thickness of 650 m, an average thickness of 760 m and a maximal thickness of 890 m.

Reservoir properties

The reservoir properties of the Lower Carboniferous Limestone Group are discussed in the corresponding section for the Bree case. In general, the Lower Carboniferous lime- and dolostones have moderate to excellent reservoir properties for geothermal up to about 2500 m. Below that depth, good reservoir conditions can be present in places with high secondary porosity, e.g., due to fracturing and/or dissolution.

Geothermal potential

Figure 13 shows the expected thermal output of a geothermal doublet that targets an area with average to high secondary permeability at a depth of 2500 to 5000 m. ‘Average secondary permeability’ refers to the value calculated from the power model shown in Figure 12. ‘High secondary permeability’ refers to the upper 95% confidence limit.

Below 4000 m, the p10 value of the predicted thermal output drops below 10 MW. Based on these results and based on the current knowledge about the reservoir properties of the Lower Carboniferous Limestone Group, 3500 m is taken as the depth limit for geothermal projects targeting the lime- and dolostones. The top of the Lower Carboniferous Limestone Group in the study area lays below the depth limit. For this reason, the limestones are not further considered as geothermal reservoir in this study.

4.4 Options for energy cascading in Lommel

Based on the evaluation of the properties of the possible geothermal reservoir units, the Triassic sandstones form the most likely target in the study area. The expected production temperature of a geothermal system targeting the sandstone varies from 32°C in the west-southwest to 56°C in the northeast. As the production temperature is below 65°C, the options for energy cascading are limited. Low temperature heating is an option, but for domestic district heating or other applications the temperature needs to be lifted using heat pumps. As the systems' efficiency goes down with the temperature lift that is needed, we restrict the current evaluation to the supply of heat for district heating. The supply temperature of the heating grid was set at 65°C and a return temperature of 45°C. So, only low temperature heating can be covered by geothermal.

The options for heat delivery and cascading were calculated from maps about geothermal potential and the heat demand in the study area using a spatial modelling tool that was developed by VITO in the context of the Flemish ERDF project 910: Geothermie 2020 (Vranckx et al., 2015). A description of the model is given in the corresponding section for the Bree case.

4.5 Blueprint for geothermal district heating design in Lommel

Figure 14 shows the general layout of the low-temperature geothermal heating plant. The blueprint is discussed in the corresponding section for the Bree case.

4.6 Techno-economic feasibility of geothermal district heating in Lommel

The techno-economic model that was used to assess the feasibility of low-temperature geothermal district heating at Lommel is the same as that used in the Bree case. The model is discussed in the corresponding section for the Bree case.

4.7 Results of the spatial optimization model

Figure 26 and Figure 27 show the results of the techno-economic spatial optimization for Lommel using two different assumptions for the heat price: a low scenario with a heat price of 40 Euro/MWh and a high scenario with a heat price of 100 Euro/MWh.

In the low scenario, the model places 2 profitable geothermal installations. The most profitable geothermal plant is placed in the north of the area and provides heat to De Vossemeren. The second plant is placed in the south and supplies heat to several industrial users on Kristalpark.

In the high scenario, the optimization tool finds 8 profitable locations for geothermal plants. Next to the two geothermal plants that were placed in the low scenario, geothermal plants are placed that provide heat to industrial users at Nolimpark and Maatheide. Some of the heating networks even extend into the neighboring municipalities of Mol, Leopoldsburg and Pelt.

The results indicate that only large consumers are connected, and few 'clusters' are connected (only small clusters of different large consumers). The choice to connect clusters is mainly dictated by the cost price of the construction of such a heat network: in case there is a cluster of, for example, office buildings and houses, the modeled heat network is calculated in such a way that

there is 1 connection from the center of the cluster to the geothermal plant and then all grid cells belonging to the cluster are connected. The necessary length of the heat network is determined by the surface area of the cluster multiplied by 140 m heat network per hectare. Connecting a cluster with several small heat consumers results in a high cost for the heating network. For example, the cost for the network connected to the geothermal plant at Nolimpark is estimated at 6.57 Meuro. In the high scenario, the cost is compensated by the demand of few customers with a moderately high heat demand (> 1,000 MWh). For clusters that only contain small users (e.g., houses), the cost for the heating network are too high to result in profitable cases. These cases only become profitable in case the sales price for the heat is above 100 Euro/MWh, or in case if social actors are willing to bear part of the investments.

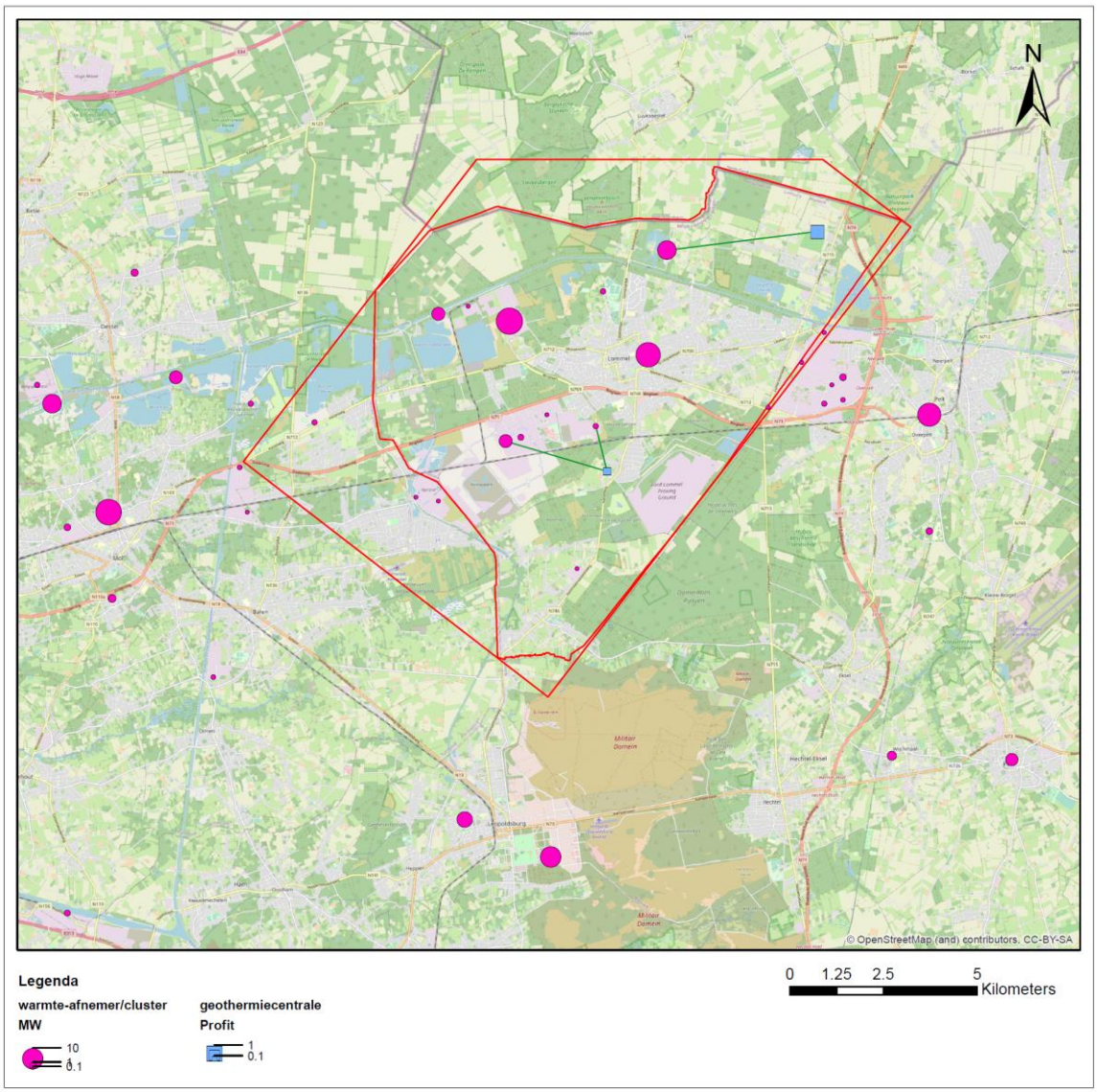

Figure 26: Result of the techno-economical optimization for locating profitable geothermal plants in the Lommel area based on a heat price of 40 Euro/MWh

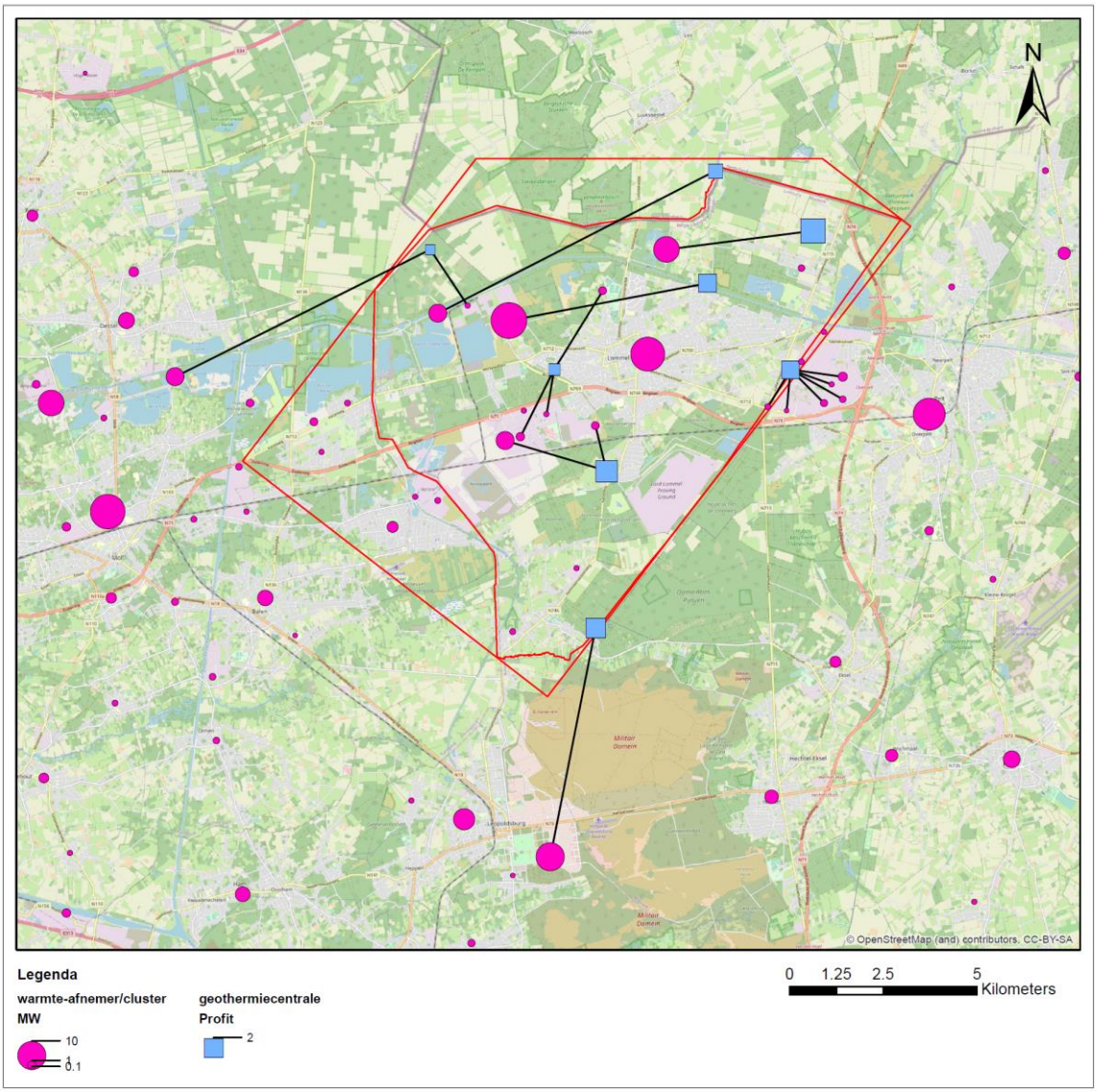

Figure 27: Result of the techno-economical optimization for locating profitable geothermal plants in the Lommel area based on a heat price of 100 Euro/MWh

5. Conclusions

5.1 Geothermal potential

Bunstandstein Formation

The main geothermal target in Bree and Lommel are porous sandstones of the Lower Triassic Buntsandstein Formation. In Bree, the top of these sandstones occurs at a depth that ranges from about -500 m TAW in the southwest to -2000 m TAW in the northeast. In a west-east direction, the top of the sandstones abruptly deepens across the Neeroeteren – Grote-Brogel Oost – Overpelt fault zone. The formation temperature will increase with depth: in the southwest, the formation temperature is estimated to be in the range 20 -30°C, in the northeast it reaches 65 – 70°C. In Lommel, the top of the Bundsandstein Formation is located at -800 to -1000 m TAW. Formation temperature ranges from 30°C in the southwest to about 60°C in the northeast.

In the part of the Bree area west of the Neeroeteren – Grote-Brogel Oost – Overpelt fault zone, the geothermal potential of the Buntsandstein is low to moderate, and only qualifies for low-temperature heating. East of the fault zone, the geothermal potential is moderate to high. Here, reservoir temperature is between 40 and 65°C. In Lommel, the geothermal potential of the Triassic sandstones is moderate. The moderate potential is due to the low production temperature.

Neeroeteren Formation

The Upper Carboniferous Neeroeteren formation has been marked as a geothermal resource in the northeastern part of the Belgium (Vandenberghe, 1991; Berkmans & Vandenberghe, 1998). The sandstones of the Neeroeteren Formation form a small geothermal reservoir in the northeast of the province of Limburg (Vandenberghe, 1991). In the Bree area, the top of the Upper Carboniferous occurs at -600 m TAW in the southwest to -2200 m TAW in the northeast.

In the area near Bree, the sandstones of the Neeroeteren Formation are up to 300 m thick. Based on the core data, the Neeroeteren Formation is expected to be a productive geothermal reservoir in the northeast of Limburg. However, due to the lack of data about the thickness and reservoir properties of the sandstones over a large part of the study area, the Neeroeteren Formation was not included in this evaluation.

Lower Carboniferous Limestone Group

Both in Bree and Lommel the top of the Lower Carboniferous Limestone Group is situated a depth of -4000 m TAW or more. is Below 4000 m, the p10 value of the predicted thermal output drops below 10 MW. Based on these results and based on the current knowledge about the reservoir properties of the Lower Carboniferous Limestone Group, 3500 m is taken as the depth limit for geothermal projects targeting the lime- and dolostones. For this reason, the limestones were not further considered in the evaluation.

5.2 Options for energy cascading

The most likely geothermal target in Lommel and Bree are the Triassic sandstones. As the expected production temperature of a geothermal system targeting these sandstones is below 65°C, the options for energy cascading are limited. Low temperature heating is an option, but in most cases the temperature needs to be lifted using heat pumps, even for domestic district heating. The use of geothermal hence is expected to be as a heat source for district heating and applications that need low temperature heat.

A typical geothermal plant targeting the Triassic sandstones will use a heat-pump to lift the temperature of the geothermal brine that reached the heat exchanger to the application temperature. For the current evaluation we considered geothermal district heating with a supply temperature of 65°C and a return temperature of 45°C. In case the geothermal brine is hot enough, a pre-heater (additional heat exchanger) is included to increase the temperature of the return before it enters the heat pump.

The preferred locations for geothermal plants were defined using a spatial optimization model developed by Vranckx et al. (2015) and a cost model for the typical geothermal plant. For each possible location, the model calculates the costs and benefits of supplying heat on an annual basis over the lifetime of a project. The project lifetime was set at 30 years. The result is a map showing locations for profitable geothermal plants and connecting them to heat users.

The benefits of the geothermal plants correspond to the revenues from the delivered heat. In this study, two scenarios were considered: a low scenario with a heat price of 40 Euro/MWh, and a high scenario with a heat price of 100 Euro/MWh.

In the low scenario, the optimization tool finds profitable locations for a geothermal plant in both Lommel and Bree. All profitable cases couple a geothermal plant with one or a few large heat users (> 2,000 MWh/year). The most profitable plants are connected to the holiday parks De Vossemeren and Erperheide. In case the heat demand is high enough, the geothermal plant can be located at a preferred geological location at several kilometers distance.

In the scenario with a heating price of 100 Euro/MWh, more profitable geothermal plants are placed. Most of the geothermal plants are connected to one or a few industrial users with a high to moderate heat demand (> 1,000 MWh/year). In addition, cases for geothermal district heating appear in the centers of Bree, Bocholt and Meeuwen. However, for clusters that only contain small heat users (e.g., houses), the cost for the heating network in most cases is too high to result in profitable cases.

6. References

Berckmans A. & Vandenberghe N., 1998. Use and potential of geothermal energy in Belgium. Geothermics 27: 235-242.

Bertier, P., Swennen, R., Laenen, B., Lagrou, D., Dreesen, R., 2006. Experimental identification of CO 2–water–rock interactions caused by sequestration of CO 2 in Westphalian and Buntsandstein sandstones of the Campine Basin (NE-Belgium). Journal of Geochemical Exploration – Journal of Geochemical Exploration 89. 10-14. 10.1016/j.gexplo.2005.11.005.

Bertier P., Swennen R., Lagrou D., Laenen B., Kemps R, 2008. Palaeo-climate controlled diagenesis of the Westphalian C & D fluvial sandstones in the Campine Basin (north-east Belgium). Sedimentology 55: 1375-1417. https://doi.org/10.1111/j.1365-3091.2008.00950.x

Bertier, P., Swennen, R., Kemps, R., Laenen, B., Dreesen, R., 2022. Reservoir characteristics and diagenesis of the Buntsandstein sandstones in the Campine Basin (NE Belgium). Geologica Belgica, Vol. 25/3-4, 145–184. https://doi.org/10.20341/gb.2022.004

Broothaers M., De Koninck R., Laenen B., Matthijs J. & Dirix K. (2020). Compilatie en duiding van warmtedata in de diepe ondergrond van Vlaanderen en opmaak van een warmtefluxkaart. 2020/RMA/R/2127 - Rapport in opdracht van de Vlaamse Overheid. Departement Omgeving.

Broothaers M., Lagrou D., Laenen B., Harcouët-Menou V., Vos D., 2021. Deep geothermal energy in the Lower Carboniferous carbonates of the Campine Basin, northern Belgium: An overview from the 1950's to 2020. Z. Dt. Ges. Geowiss. (J. Appl. Reg. Geol.), 172 (3), p. 211–225; https://doi.org/10.1127/zdgg/2021/0285

Cardwell W.T., Parson R.L, 1945. Average Permeabilities of Heterogeneous Oil Sands. T.P. 18S2 in Petroleum Technology. March 1945: 34-42.

Deckers J., Vernes R., Dabekaussen W., Den Dulk M., Doornenbal D., Dusar M., Hummelman J., Matthijs J., Menkovic A., Reindersma R., Walstra J., Westerhoff W. & Witmans N., 2014. Geologisch en hydrogeologisch 3D model van het Cenozoïcum van de Roerdalslenk in Zuidoost-Nederland en Vlaanderen (H3O – Roerdalslenk). Studie uitgevoerd in opdracht van: Afdeling Land en Bodembescherming, Ondergrond, Natuurlijke Rijkdommen van de Vlaamse Overheid, Afdeling Operationeel Waterbeheer van de Vlaamse Milieumaatschappij, Nederlandse Provincie Limburg, Nederlandse Provincie Noord-Brabant. VITO-rapport 2014/ETE/R/1

Dupont, H., 1992. Sedimentpetrologische studie van de Neeroeteren Zandsteen (Westfaliaan D) (Boring 172 van het Kempens Bekken). Master Thesis, KU Leuven.

Dusar M. & Houlleberghs E., 1981. De steenkoolverkenningsboring van Neerglabbeek (Boring 146 van het Kempens bekken). Annales des Mines de Belgique, 11/1981: 913-992.

Haslego, C. & Polly, G., 2002. Compact heat exchangers: part 1. CEP Magazine September 2002, p. 32-37.

Dusar, M., Langenaeker, V. & Wouters, L., 2001. Permian – Triassic – Jurassic lithostratigraphic units in the Campine basin and the Roer Valley Graben (NE Belgium). Geologica Belgica, 4, 107-112.

Heederik J.P., Brugge J., Brummer C.H., Coenegracht Y.M.A., van Doorn T.H.M., Huurdeman A.J.M., Van Gaans P.F.M., Vasak L., Vierhout R.M. & Zuurdeeg B.W., 1989. Geothermische reserves Centrale Slenk, Nederland. Exploratie en evaluatie. TNO Rapport OS 89-18.

Ingebritsen S.E., Manning, C.E., 1999. Geological implications of a permeability-depth curve for the continental crust. Geology; v. 27; no. 12; p. 1107–1110.

Laenen, 2001. Lithostratigrafie van het pre-Tertiair in Vlaanderen. Deel I: post-Dinantiaan. Studie uitgevoerd in opdracht ANRE, VITO-rapport 2002/ETE/R/063; Lithostratigrafie van het pre-Tertiair in Vlaanderen. Deel I: post-Dinantiaan | Vlaanderen.be

Laenen, 2003. Lithostratigrafie van het pre-Tertiair in Vlaanderen. Deel II: Dinantiaan & Devoon. Studie uitgevoerd in opdracht ANRE, VITO-rapport 2003/ETE/095; Lithostratigrafie van het pre-Tertiair in Vlaanderen. Deel II: Dinantiaan & Devoon | Vlaanderen.be

Laenen B., Broothaers M., van Tongeren P., Ferket H., 2008. Exploratie van Noordoost Limburg. Fase 1: Acquisitie, processing en interpretatie van de 2D seismische campagne Bree - Kinrooi – Maaseik. Studie in opdracht van VITO. VITO-rapport 2008/MAT/R/063.

Langenaeker, V.: The Campine Basin: stratigraphy, structural geology, coalification and hydrocarbon potential of the Devonian to Jurassic, Aardkundige Mededelingen, 10, (2000), 1-142.

Larionov, V.V. (1969), Radiometry of Boreholes, NEDRA, Moscow.

Lemmond, E.W., Bell, I. H., Huber, M. L., McLinden, O.M., 2018. REFPROP Documentation, release 10.0. https://www.nist.gov/system/files/documents/2018/05/23/refprop10a.pdf

Lingen, 2015a. Analysis of Welltest BRI-GT-01. PanTerra Geoconsultants B.V., report prepared for HydrecoGeoMEC. NLOG_GS_PUB_Well Test Analysis BRI_GT-01.pdf

Lingen, 2015b. Analysis of Welltest BRI-GT-02. PanTerra Geoconsultants B.V., report prepared for HydrecoGeoMEC. NLOG_GS_PUB_Well Test Analysis BRI_GT-02.pdf

Milius G., 1983. Inventarisatie van de Lower Trias Group in Nederland t.b.v. de winning van Aardwarmte. Onderzoek uitgevoerd in opdracht van het Projectbureau Energieonderzoek van TNO, in het kader van bet Nationaal Onderzoekprogramma Aardwarmte — project no. 90740.030; Rijks Geologische Dienst, Report no. 82D52J; https://www.nlog.nl/sites/default/files/1982%2082ds21%20inventarisatie%20lower%20trias%20group%20t.b.v.%20aardwarmte.pdf

Patyn, J., 1999. Boring Meeuwen: interpretatie puttesten Trias (Bundsandstein). VITO-nota - Patyn J. 1999 - DIA/G1000/JP/jp/99-033.

Renard Ph., de Marsily G., 1997. Calculating equivalent permeability: a review. Advances in Water Resources 20: 253-278.

Rocco, E., Harcouët-Menou, V., Venturin, A., Guglielmetti, L., Facco, L., Olivieri, N., Laenen, B., Caia V., Vela, S., De Rose, A., Urbano, G., Strazza, C., 2020. Study on 'Geothermal plants' and applications' emissions : overview and analysis : final report. Study ordered by the Directorate-General for Research and Innovation (European Commission). https://doi.org/10.2777/755565

Rossa, H.G., 1986. Upper Cretaceous and Tertiary inversion tectonics in the western part of the Rhenish-Westphalian coal District (FRG) and in the Campine area (Belgium). Annales de la Société géologique de Belgique. 367-410.

Swennen, R., Dusar, M., 1997. Diagenesis of Late Cretaceous to Paleocene carbonates in the Rur Valley Graben (Molenbeersel borehole, NE-Belgium). Annales de la Société géologique du Nord, vol. 5(3): 215-226.

Vandenberghe, N., 1991: Belgium. - In: Geothermal Atlas of Europe (Eds.: Hurtig, E., Cermak, V., Haenel, R. and Zui, V.), Hermann Haack Verlagsgesellschaft, Gotha, Germany, p. 14-15.

Vranckx S., Van der Meulen M., Poelmans L., Uljee I., Engelen G., Lagrou D., Laenen B., 2015. Eindrapport EFRD-project geothermie: Ruimtelijke Inplantingsanalyse. VITO-rapport RMA/1410166/2015-0001.

Wouters, L., Gullentops, F., 1988. The sedimentology of the Westphalian D Neeroeteren sandstone, Kempen (Belgium). Ann. Soc. Géol. Nord, CVII: 191 – 202.

Wyllie, M. R. J., Gregory, A. R., and Gardner, L. W., 1956, Elastic wave velocities in heterogeneous and porous media: Geophysics, 21, no. 1, 41-70.

ANNEX 1: Estimated flow rates for the Triassic sandstones

Estimated flow rates for the Bree Member and Nederweert equivalent in Bree

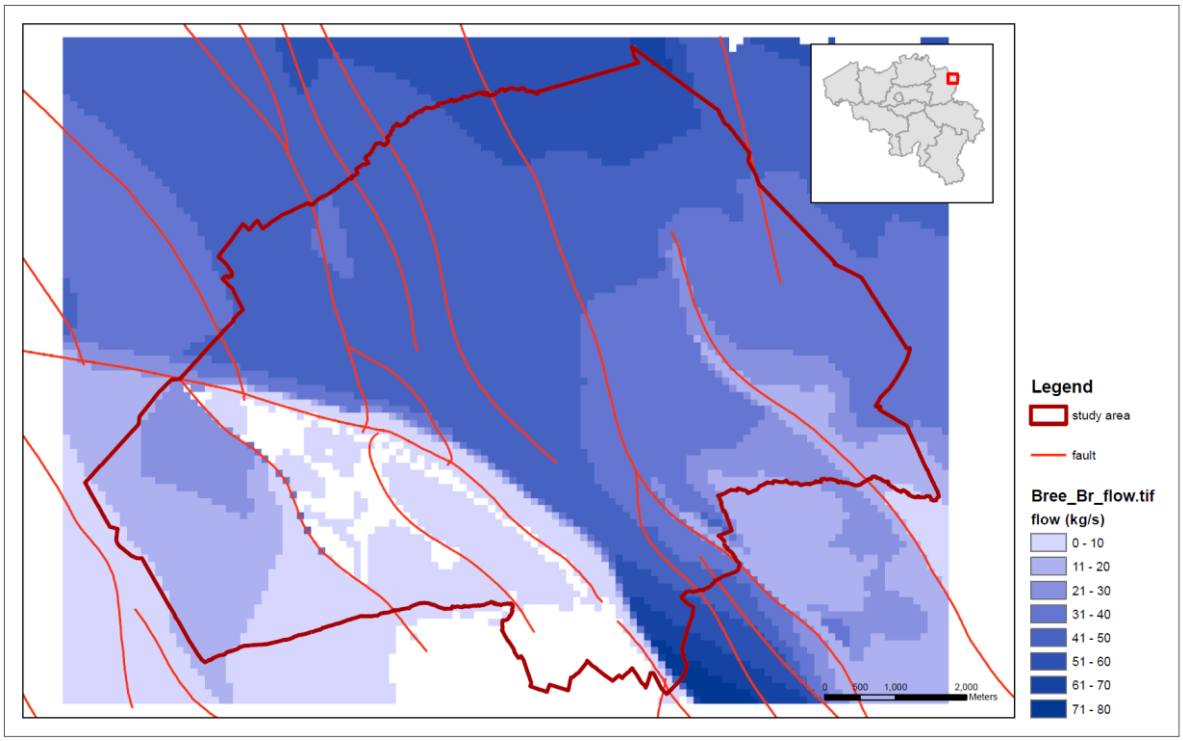

Figure 28: Estimated average flow rate of a geothermal doublet targeting the Bree Member

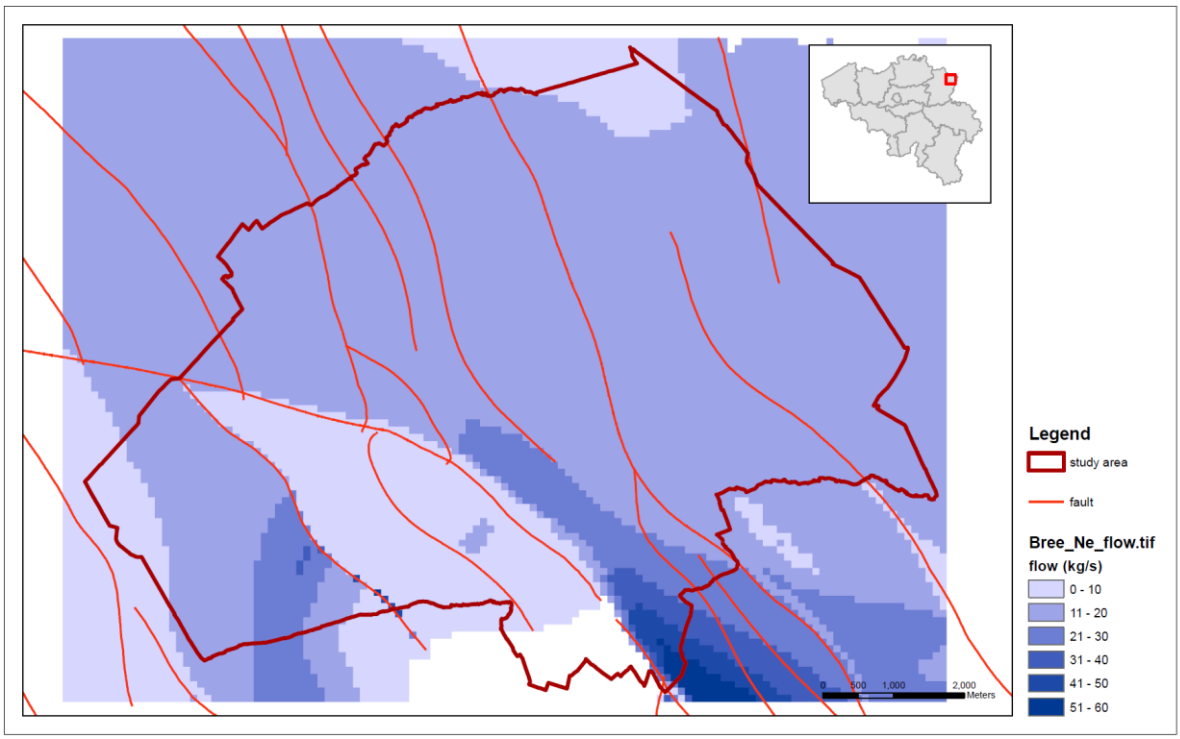

Figure 29: Estimated average flow rate of a geothermal doublet targeting the Nederweert equivalent

Estimated flow rates for the Bree Member and Nederweert equivalent in Lommel

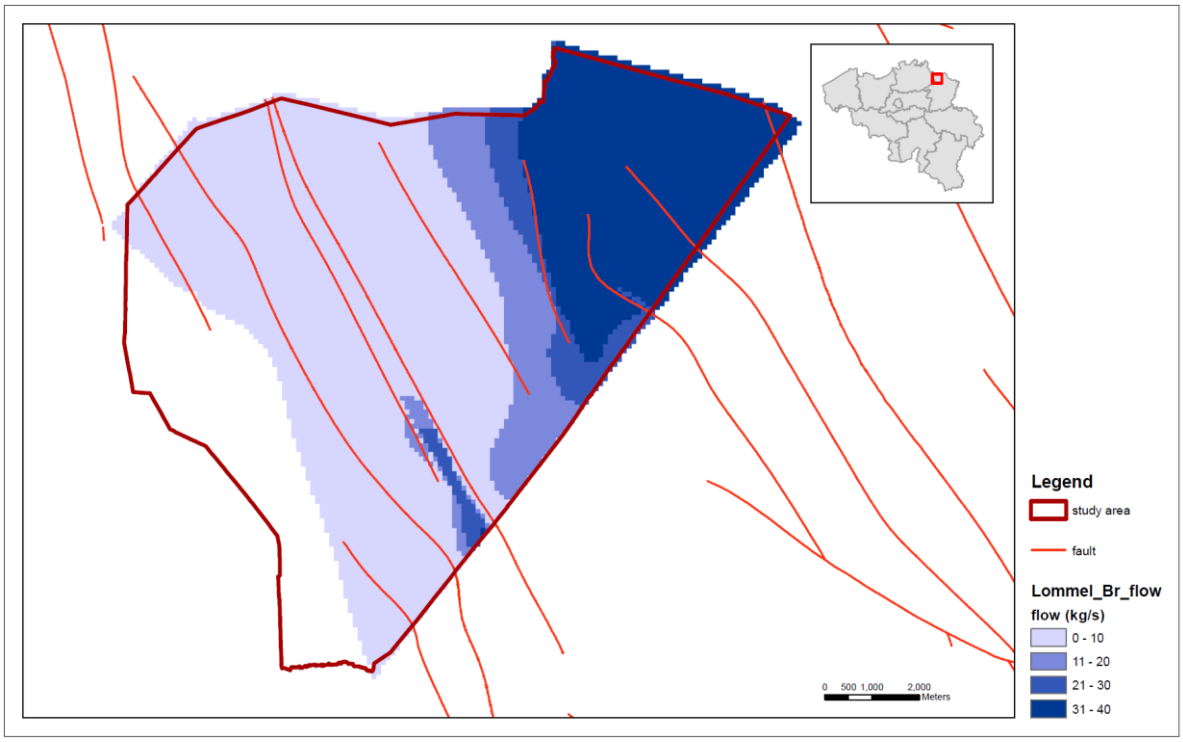

Figure 30: Estimated average flow rate of a geothermal doublet targeting the Bree Member

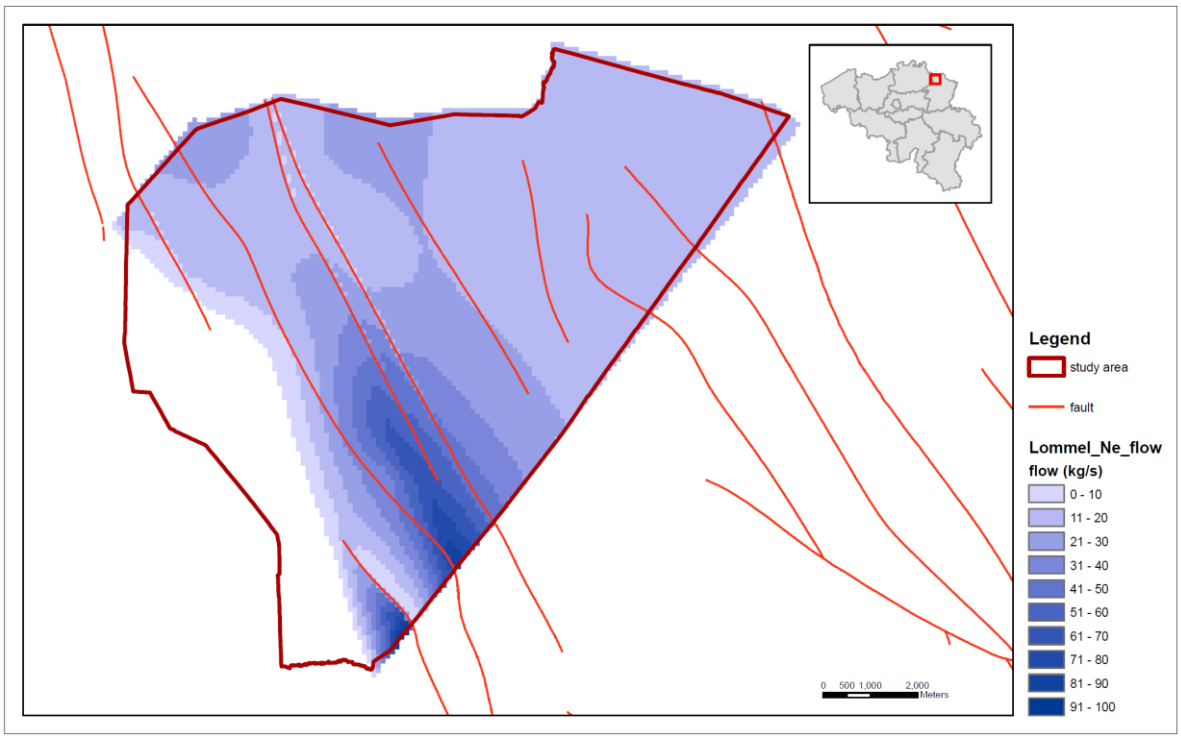

Figure 31: Estimated average flow rate of a geothermal doublet targeting the Nederweert equivalent

ANNEX 2: Estimated formation temperature for the Triassic sandstones

Estimated formation temperatures in the Bree study area

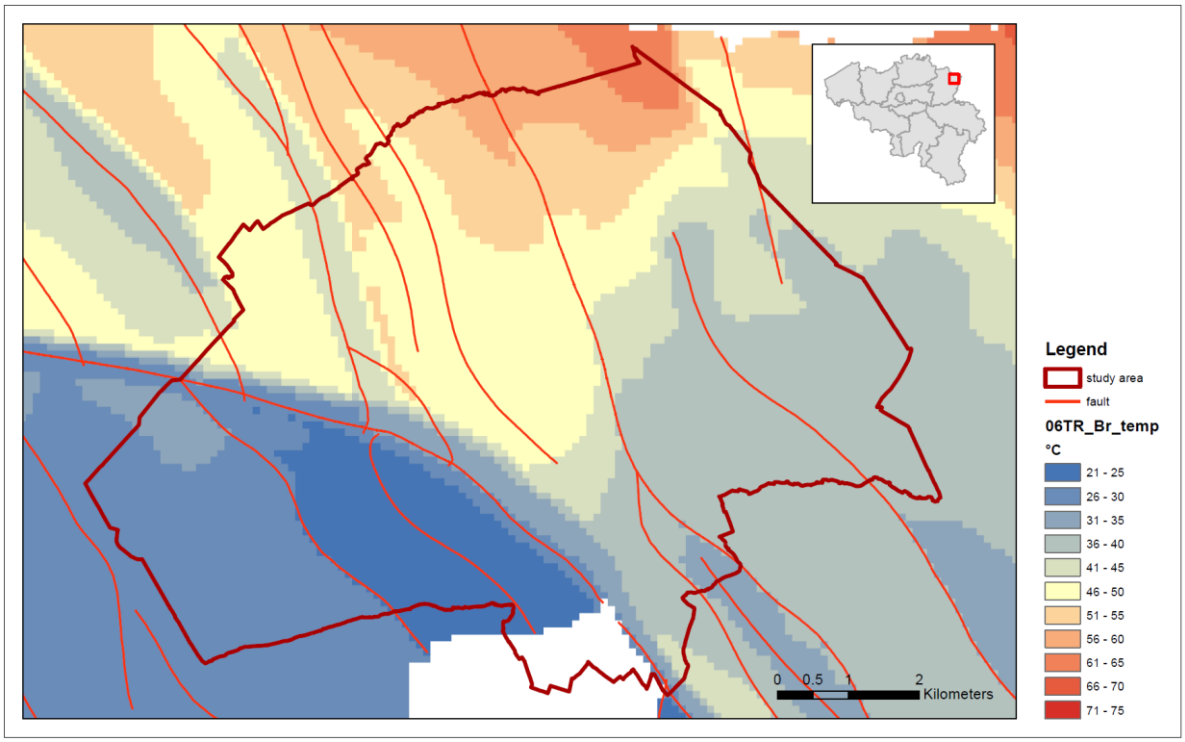

Figure 32: Estimated average formation temperature of the Bree Member at Bree

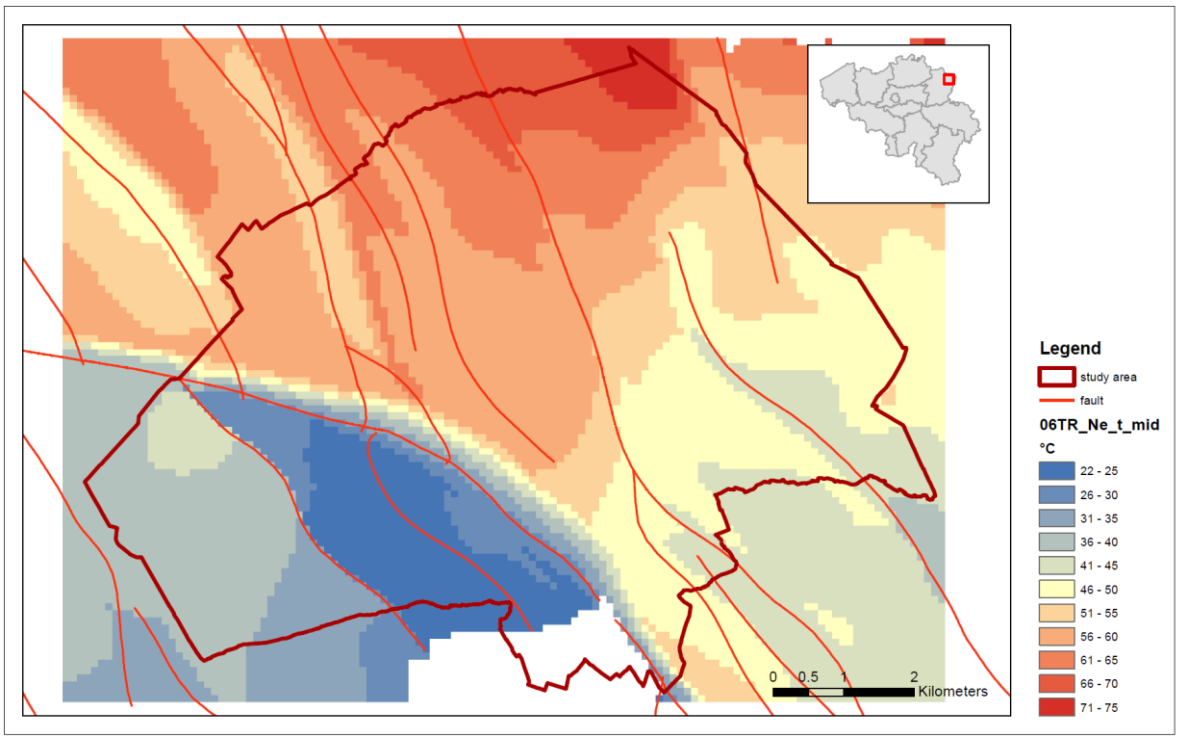

Figure 33: Estimated average formation temperature of the Nederweert equivalent at Bree

Estimated formation temperatures in the Lommel study area

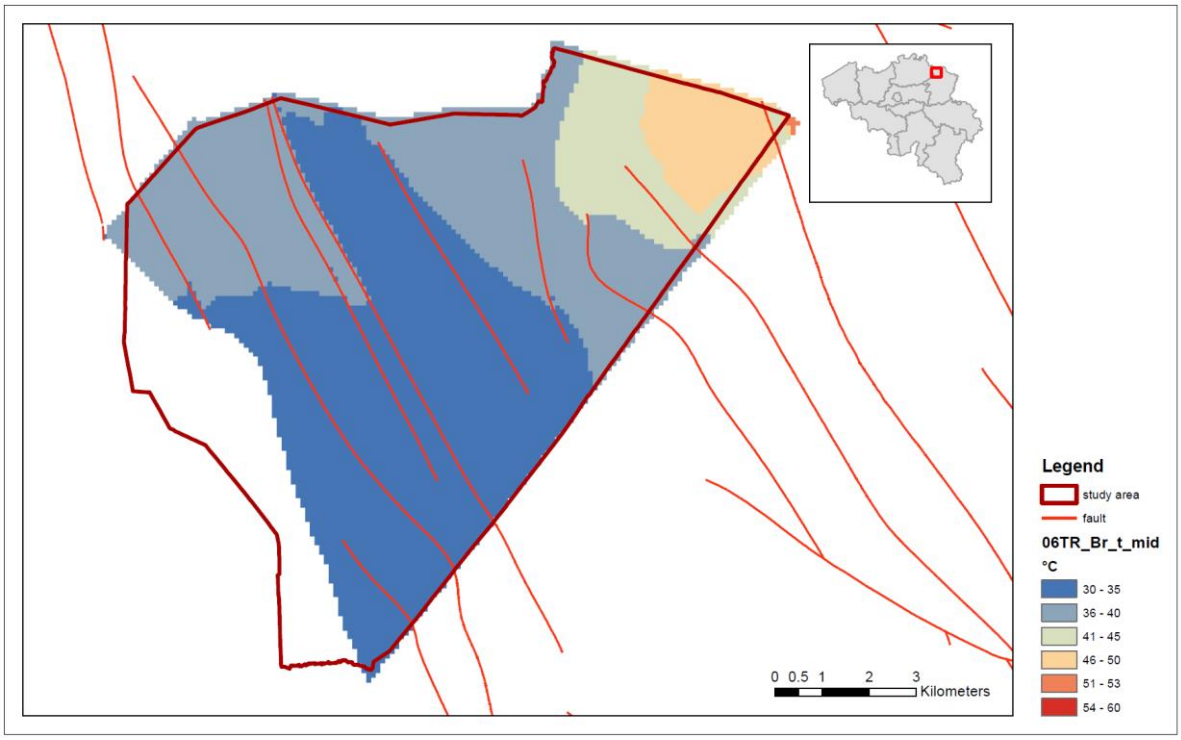

Figure 34: Estimated average formation temperature of the Bree Member at Bree

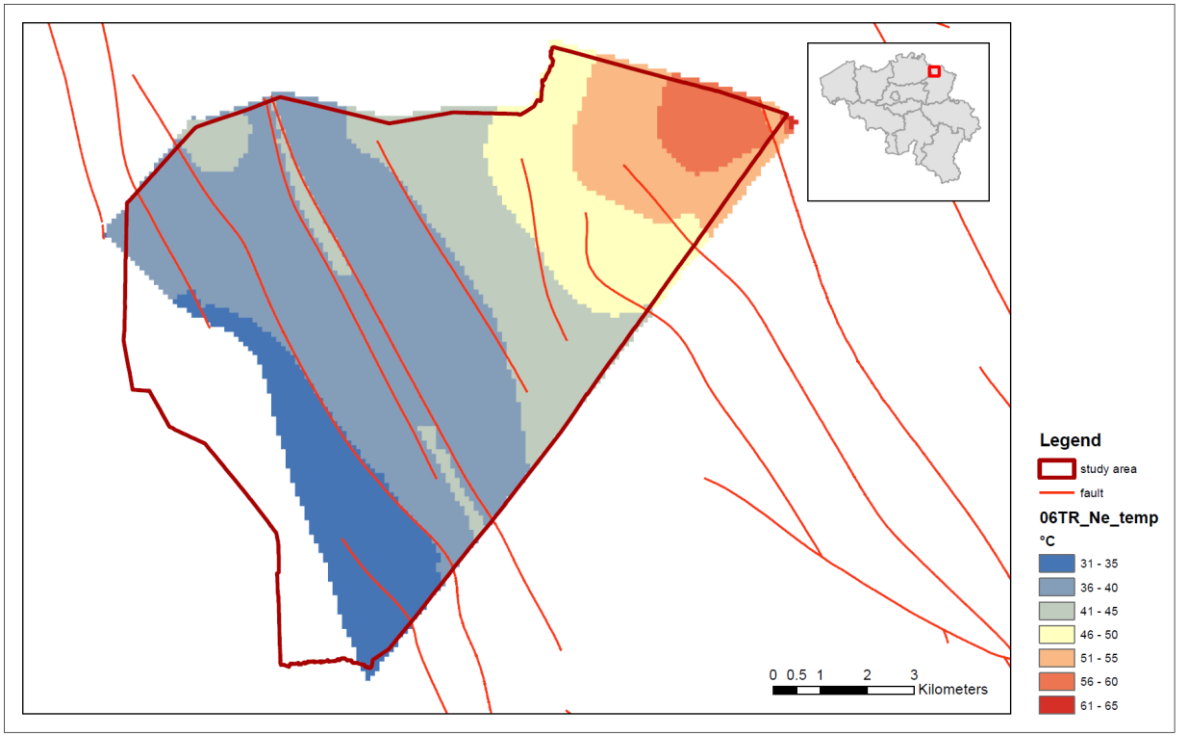

Figure 35: Estimated average formation temperature of the Nederweert equivalent at Lommel